Expert Systems With Applications 72 (2017) 1–17

Contents lists available at ScienceDirect

Expert Systems With Applications

journal homepage: www.elsevier.com/locate/eswa

A novel mobile robot localization approach based on topological maps using classification with reject option in omnidirectional images

Leandro B. Marinho[a], Jefferson S. Almeida[a], João Wellington M. Souza[a], Victor Hugo C. Albuquerque[b], Pedro P. Rebouças Filho[a,*]

[a] Laboratório de Processamento de Imagens e Simulação Computacional, Instituto Federal de Educação, Ciência e Tecnologia do Ceará, Maracanaú, CE, Brazil
[b] Programa de Pós-Graduação em Informática Aplicada, Universidade de Fortaleza, Fortaleza, Ceará, Brazil

ARTICLE INFO

Article history:
Received 23 June 2016
Revised 27 October 2016
Accepted 5 December 2016
Available online 6 December 2016

Keywords:
Robot visual localization
Omnidirectional camera
Feature extraction
Pattern recognition
Topological map

ABSTRACT

Mobile robot localization, which allows a robot to identify its position, is one of main challenges in the field of Robotics. In this work, we provide an evaluation of consolidated feature extractions and machine learning techniques from omnidirectional images focusing on topological map and localization tasks. The main contributions of this work are a novel method for localization via classification with reject option using omnidirectional images, as well as two novel omnidirectional image data sets. The localization system was analyzed in both virtual and real environments. Based on the experiments performed, the Minimal Learning Machine with Nearest Neighbors classifier and Local Binary Patterns feature extraction proved to be the best combination for mobile robot localization with accuracy of 96.7% and an Fscore of 96.6%.

1. Introduction

Interest in autonomous mobile robots is increasing along with the advancements in technology being made. Mobile robots have been widely applied to military and civilian tasks. In Bengochea-Guevara, Conesa-Muñoz, Andújar, and Ribeiro (2016), the authors presented an example of an autonomous robot in precision agriculture. Song, Gao, Ding, Deng, and Chao (2015) used a mobile robot to identify terrain parameters. Miksik, Petyovsky, Zalud, and Jura (2011) presented an unmanned ground vehicle that can be used for nuclear, chemical and biological contamination measurements among other applications.

Mobile robot mapping and localization methods can be grouped into two central paradigms (Enrico, Groen, Arai, Dillmann, & Stenz, 2000): (i) geometric, such as Arbeiter, Bormann, Fischer, Hägele, and Verl (2012); Nagla, Uddin, and Singh (2012); Zhang, Liu, and Tan (2015), and (ii) topological, such as Chin, Loo, Seera, Kubota, and Toda (2016); Dawood and Loo (2015); Gerstmayr-Hillen et al. (2013); Hafez and Loo (2015). Geometric maps represent the total navigation space in a global coordinate system. Instead of focusing on stiff geometric information, topological methods represent the environment as a graph. The vertexes are locations in the environment and are connected by arches, if there is a path between them Rady (2016); Wu, hui Tian, Li, yu Zhou, and Duan (2014). Topological maps are useful for mobile robot localization tasks. These kinds of maps are compact and simple, require less computer memory, and consequently speed up robot navigation processes (Cheng, Chen, & Liu, 2015). Other methods are a combination of both geometric and topological methods. Good examples of this hybrid approach are presented in Rady (2016); Wu et al. (2014).

In the outdoor environment, navigation systems such as the Global Positioning System (GPS) provide precise positions and can be applied in mobile robot localization. However, in an indoor environment it is difficult for GPS to supply accurate positioning information. In the latter environments, different positioning methods have been proposed, such as the ultrasound, Bluetooth, Wi-Fi, image recognition and inertial navigation (Song, Jiang, & Huang, 2011; Xu, Chen, Xu, & Ji, 2015; Zhu, Yang, Wu, & Liu, 2014). Yayan, Yucel, and Yazıcı (2015) presented an indoor positioning system that uses ultrasonic signals and calculates the position of the mobile robot. Nevertheless, this type of positioning system suffers from small noise sources such as jangling metal objects. A method for mobile robot localization in a partially unknown indoor environment which merge ultrasonic sensors with a laser range finder (LRF) was proposed in Ko and Kuc (2015). Nevertheless, the usage of expensive sensors for the identification is the main drawback of the LRF. Song, Li, Tang, and Zhang (2016) presented a positioning

* Corresponding author.
E-mail addresses: leandro.marinho@ppgcc.ifce.edu.br (L.B. Marinho), jeffersonsilva@lapisco.ifce.edu.br (J.S. Almeida), wellmendes@lapisco.ifce.edu.br (J.W.M. Souza), victor.albuquerque@unifor.br (V.H.C. Albuquerque), pedrosarf@ifce.edu.br (P.P. Rebouças Filho).

http://dx.doi.org/10.1016/j.eswa.2016.12.007
0957-4174/

system with Radio-Frequency Identification (RFID). However, the system needs a complex infrastructure in the environment.

Mobile robot vision-based navigation has been extensively studied in computational vision and control and automation engineering (Wang, Cai, Yi, & Li, 2012). The images captured by a vision-based system need to be described and compared to carry out mapping and localization tasks. The description technique used can be based on global descriptors, on local features, on Bag-Of-Words (BoW) schemes, see Li, Dong, Xiao, and Zhou (2016), or based on combined approaches (Garcia-Fidalgo & Ortiz, 2015). Woo, Lim, and Lee (2010) proposed a system that combines global with local features to identify pedestrians and vehicles. Aldana-Murillo, Hayet, and Becerra (2015) used local descriptors in the problem of appearance-based localization.

Global descriptors are usually effective to solve the computational needs during mapping and localization tasks. However, solutions based on global representation (different fields of knowledge) suffer from problems such as occlusions or camera rotations. These issues have been widely discussed with the current advancement of local features (Garcia-Fidalgo & Ortiz, 2015). Khan, Ahmed, and Khan (2013) presented a solution for a surveillance problem using image moments and artificial neural networks. Boroş, Roşca, and Iftene (2010) applied Scale Invariant Feature Transform (SIFT) to solve the problem of global topological localization for indoor environments. In Zhang and Hua (2015), Local Binary Patterns (LBP) were used to face the detection task. Raheja, Kumar, and Chaudhary (2013) presented a system to detect fabric defects using Gray Level Co-occurrence Matrix (GLCM). These methods are effective in scene recognition due to their properties of building new features that are powerfully related to the output class.

Machine learning methods have been widely applied along with computer vision techniques into mobile robot navigation systems due their effective capacity of learning complex patterns and making decisions based on data (Yang, Shao, Zheng, Wang, & Song, 2011a). Charalampous, Kostavelis, and Gasteratos (2015) presented a local path planning method, incorporating the support vector machines (SVM) algorithm. Caron, Filliat, and Gepperth (2015) used a feed-forward neural network along with a RGB-D camera for object recognition. In Kasat and Thepade (2016), an image classification approach was proposed using Bayes classifier.

Some applications require high performance (high accuracy and short processing time) through convectional cameras. Omnidirectional vision systems have been widely used because they increase the amount of information available. A system with a panoramic view provides a 360° image, that may be necessary, for example, when the task performed by the robot needs to have constant visual information of objects in different places (Scaramuzza, 2014). Kim and Kweon (2013) presented a paradigm of a global localization method using an omnidirectional camera. In Maohai, Han, Lining, and Zesu (2013), a topological navigation strategy for an omnidirectional mobile robot using an omnidirectional camera was described.

The aim of this work is to provide an evaluation of consolidated feature extractions and machine learning techniques in omnidirectional images focusing on a topological map and mobile robot localization tasks. In this work, a new and robust method for localization via classification with option using omnidirectional images was developed and analyzed. Initially, the navigation system was analyzed with images generated from a virtual environment. Posteriorly, the same perception module based on a vision sensor was used in a real environment with an omnidirectional camera. The developed systems were able to recognize the navigable area of the environments by processing the input data and to classify them into states which represent the current robot context. These capabilities allowed the robots to determine their localization on a topological map and also to autonomously navigate through the environment, reaching the desired destination. Results show that the Minimal Learning Machine with Nearest Neighbors (MLM-NN) is a promising classifier for the analytical task. In addition, the experiments demonstrated that LBP was the best feature extraction technique for this task.

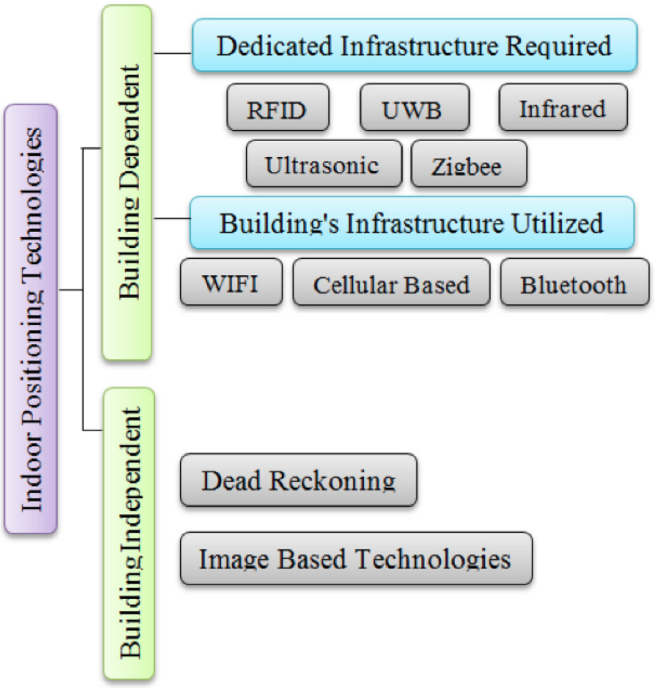

Fig. 1. Categorization of indoor positioning technologies (Alarifi et al., 2016).

2. Related work

Localization requires a robot to estimate its position in the environment. This is a basic ability for any navigation task (Castellanos & Tardos, 2012). Thus, the localization system must acquire the largest amount of information concerning the environment as possible. There are numerous types of sensors used in mobile robotics for this task and among them are technologies based on ultrasound, on laser or based on computer vision (Deak, Curran, & Condell, 2012). Alarifi et al. (2016) classified indoor positioning technologies according to the infrastructure of the system that uses them, see Fig 1. Table 1 compares the advantages and disadvantages of these technologies and indicates some studies related to these technologies. There are numerous advantages of using a localization method based on computer vision. They are easily scalable without significant increase of costs, and they do not demand changing the environment (Mautz & Tilch, 2011).

Garcia-Fidalgo and Ortiz (2015) reviewed several approaches with regard to topological mapping and localization by visual means. The authors classify these approaches into global descriptors, local features, or Bag-Of-Words (BoW). Table 2 presents the advantages and disadvantages of each of these approaches and some applications. As shown in Table 2, there are several contributions for the use of computer vision in navigation and robot localization. Computer vision is used in the proposed approach, This work use this approach, however with two contributions, one from the scientific point of view and the other from the technological point of view.

Decision support methods have evolved to reproduce decisions similar to those made by humans. However, these methods still have errors. Thus, paradigms, which provide a more viable alternative, have been developed when the confidence in the decision is low (Gamelas Sousa, Rocha Neto, Cardoso, & Barreto, 2015). Faced

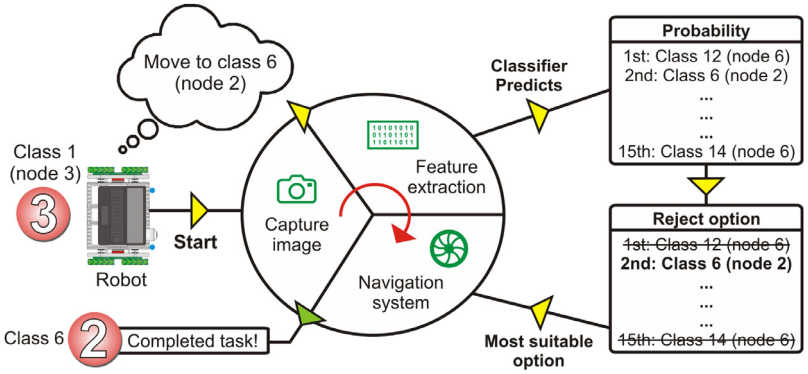

Fig. 2. A hypothetical situation in which the classifier predicts that there is a higher probability of the current position to be a place too far away from the destination.

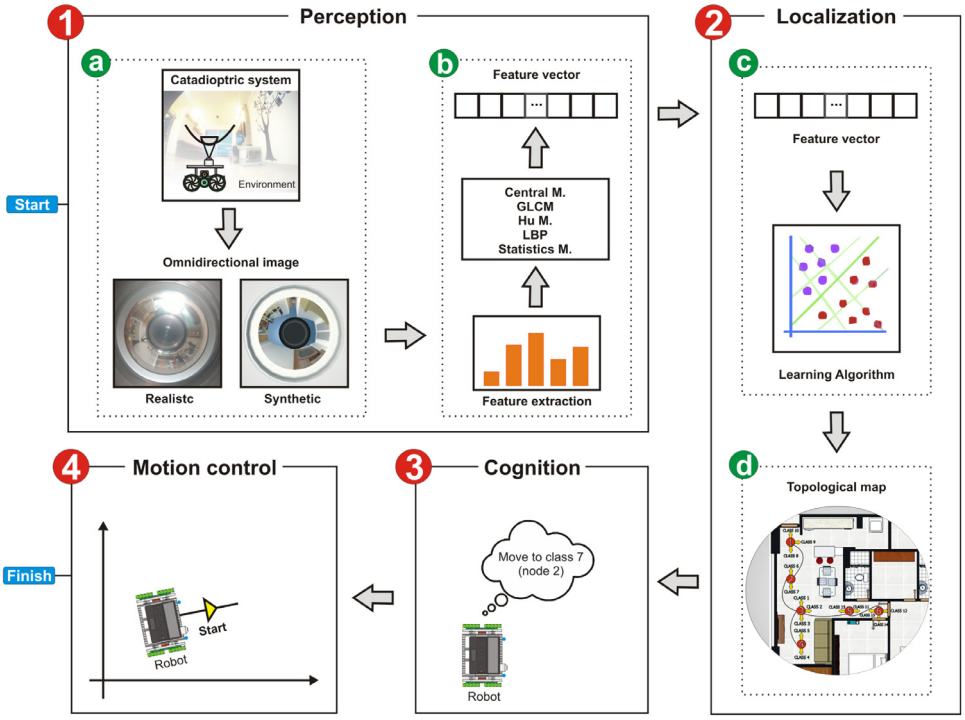

Fig. 3. Proposed system flowchart. (1) The omnidirectional image is captured and the feature vector is created through feature extraction techniques. (2) The feature vectors are presented to a classifier to perform the recognition of the environment. (3) Cognition. (4) Motion control.

(a) Top view. (b) Perspective view. (c) Robot.

Fig. 4. Topological map of the test environment: a) top; b) perspective views; and c) the autonomous mobile robot.

Table 1
Comparison among indoor localization technologies.

Technology	Common measurement methods	Advantage	Disadvantage	System
Image based technologies	Pattern recognition	They do not require changing the environment in any way (deploy RFID tag or WiFi routers, e.g.) (Deak et al., 2012); they have the potential for large scale coverage without significant increase of the costs (Mautz & Tilch, 2011).	LOS may occur (Song et al., 2011); some image processing methods require high computing costs (Hartmann, 2011).	Rubio, Martínez-Gómez, Flores, and Puerta (2016), Son, Kim, and Sohn (2015), Debski, Grajewski, Zaborowski, and Turek (2015), Li (2014).
Bluetooth	Proximity, RSS	Present in common devices such as smartphones (Deak et al., 2012); LOS is not required (Song et al., 2011).	The uses must to do a scan The users must do a scan to detect the beacons in the area (Deak et al., 2012); cover range is limited (Mainetti, Patrono, & Sergi, 2014).	(Kwiecień, Maćkowski, Kojder, & Manczyk, 2015), Li (2014).
Zigbee	RSS, Phase Shift Measurements	Low cost and energy consumption (Song et al., 2011).	Low transmission rate, complexity and cost (Alarifi et al., 2016).	Fang, Wang, Huang, Yang, and Chen (2012)
WLAN	RSS	The hardware is cost effective and easy to install; LOS is not required (Chowdhury, Elkin, Devabhaktuni, Rawat, & Oluoch, 2016).	Affected by multipath and fast fading effects (Chowdhury et al., 2016).	Nowicki and Skrzypczyński (2015), Campos, Lovisolo, and de Campos (2014), Lim, Kung, Hou, and Luo (2010)
UWB	ToA, TDOA	UWB signals have greater penetration of obstacles; it has a desirable direct resolvability of direct multipath components (Alarifi et al., 2016).	High financial cost (Song et al., 2011).	Zandian and Witkowski (2016), Monica and Ferrari (2015), Arias-de Reyna (2013).
RFID	Proximity, RSS	Suitable for dense environments; does not require LOS (Deak et al., 2012).	High cost of readers, complex infrastructure	Calderoni, Ferrara, Franco, and Maio (2015), Miah and Gueaieb (2011).
Ultrasonic	ToA, TDOA	Low cost; does not suffer interference from electromagnetic waves (Deak et al., 2012).	Affected by high frequency sounds; large scale implementation is complex (Deak et al., 2012).	Yayan et al. (2015), Kim and Choi (2008).
Infrared	Proximity, Differential Phase-shift, AoA	Absence of radio electromagnetic interference (Chowdhury et al., 2016).	Expensive system hardware and maintenance cost (Chowdhury et al., 2016).	Sioutis and Tan (2014), Schindler, Metzger, and Starner (2006).
Celluar Based	RSS	Can work at the same frequency as other devices (Deak et al., 2012).	Low precision (Deak et al., 2012).	Varshavsky, de Lara, Hightower, LaMarca, and Otsason (2007).
Dead Reckoning	Tracking	Extra hardware is not required.	Computes an approximate position (Alarifi et al., 2016)	Kothari, Kannan, Glasgwow, and Dias (2012), Jimenez, Seco, Prieto, and Guevara (2009).

Table 2
Vision-based topological schemes and solutions.

	Advantage	Disadvantage	Descriptor	References
Global descriptors	Easy to compute and save storage space; reduce the computational needs of mapping and localization tasks (Bonin-Font, Ortiz, & Oliver, 2008).	Low robustness to occlusion and illumination effects, reducing the discrimination power (Bonin-Font et al., 2008).	PCA Omni-gist DP-FACT	Bessa et al. (2015) Rituerto, Murillo, and Guerrero (2014) Liu and Siegwart (2012)
Local features	High discrimination power; they are usually more robust to changes in scale and occlusions, illumination and rotation (Garcia-Fidalgo & Ortiz, 2015)	The computational cost and the storage needs are higher than for global descriptors (Fuentes-Pacheco, Ruiz-Ascencio, & Rendón-Mancha, 2015).	SIFT Wavelets 3D-PIRF (SURF)	Johns and Yang (2011) Saedan, Lim, and Ang (2007) Morioka, Yi, and Hasegawa (2011)
BoW schemes	Satisfactory with high number of images to process (Fuentes-Pacheco et al., 2015)	There is a presence of noisy words due to the coarseness of the vocabulary construction method and the loss of the spatial relations between the words; moderate storage needs (Garcia-Fidalgo & Ortiz, 2015).	FAST/BRIEF SURF SIFT	Galvez-López and Tardos (2012) Cummins and Newman (2011) Ranganathan and Dellaert (2011)

with these challenges, we propose a novel method for localization via classification with a reject option using omnidirectional images. Our method uses distance information of the topological map to provide, automatically, a suitable option during the localization when the confidence in the decision is low. Results show that the proposed method increased the accuracy of all classifiers evaluated in this work, in other words, the classification is optimized.

The contribution of this work from the technological point of view is the use of global and local feature extraction techniques based on moments (Statistical Moments, Central Moments and Hu Moments), on texture (LBP and GLCM), and keypoint descriptor (SIFT and SURF) along with a recently developed classifier, MLM-NN, and consolidated machine learning techniques for mobile robot localization tasks with omnidirectional images. Furthermore, we asses the localization system in both virtual and real environments. As can be seen in Table 2, the other works perform a simple comparison with a few methods. In contrast, we evaluate several approaches in order to optimize the solution.

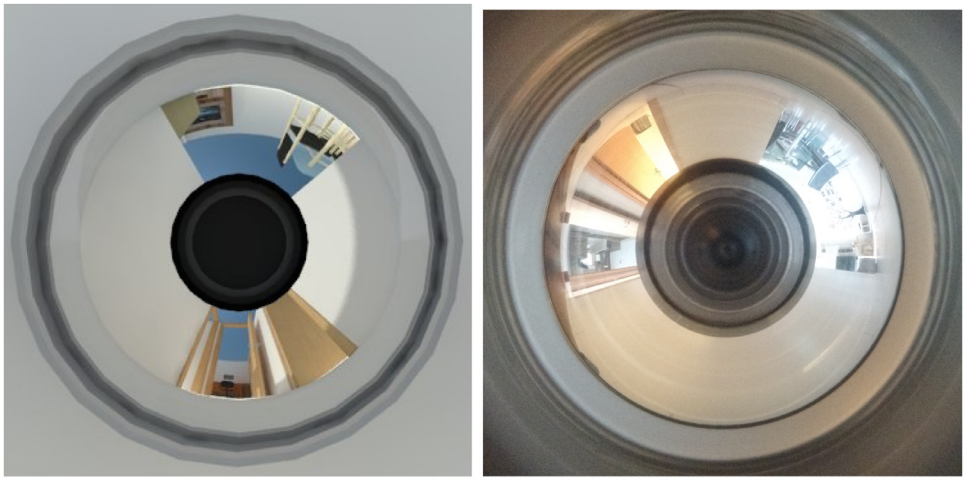

(a) Virtual environment. (b) Real environment.

Fig. 5. Class 15 in node 5 in a) virtual environment and b) real environment.

Table 3
Number of attributes generated by each feature extraction technique.

Feature extraction	Number of attributes
Central moments	7
GLCM	14
Hu	7
LBP	59
Statistical moments	10

Table 4
Commands to move the robot, as well, the start and end locations used in the route testing. Go straight ahead (GSA), turn left (TL), turn right (TR) and turn 180 degrees (T180).

Name	Start (Class)	Comands	End (Class)
1	8	GSA, GSA, GSA	4
2	1	GSA, GSA, TR	9
3	5	GSA and TR, GSA, GSA	12
4	5	GSA, GSA, GSA and TR, TL	10
5	8	GSA, GSA and TL, GSA, GSA	12
6	13	GSA, GSA and TL, GSA, T180, GSA	1
7	8	GSA, GSA, TL, GSA, GSA	12
8	9	TR, GSA, GSA and TL, GSA, T180, GSA and TL	3
9	2	GSA, GSA and TR, TR, GSA, GSA and TL	3
10	12	T180, GSA, GSA and TL, GSA, T180, GSA, GSA, GSA	10

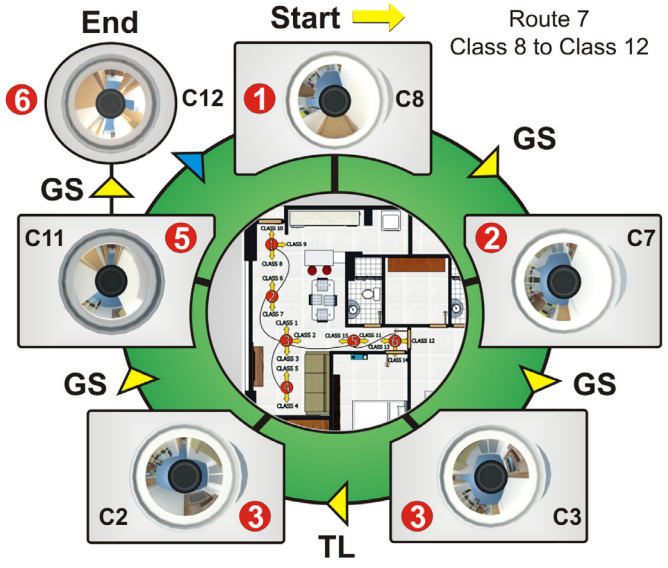

Fig. 6. Illustration of route 7. The robot begins at node 1 (class 8) and goes straight ahead twice. It turns to the left and again goes straight ahead twice. Finally, it reaches node 6 (class 12).

3. Overview of feature extraction methods

In this work, the region of interest (ROI) in an omnidirectional image will be the whole picture. From this ROI, attributes are extracted to be used for classification via machine learning techniques. The feature extraction methods are presented below.

Statistical moments are an important method used for image feature extraction. These moments describe the spatial distribution of points contained in the images or region of interest. Moments define some important measures about the object of interest that are useful to identify them (Gonzalez & Woods, 2010; Hu, 1962a). Kaushik, Bajaj, and Mathew (2015) used statistical moments to detect copy-move forgery in digital images.

According to Paul, Bhattacharya, and Chowdhury (2012a), central moments are very important in pattern recognition. They can be derived from spatial moments by reducing these moments with the center of gravity of the object (Czachorski, Kozielski, & Stanczyk, 2011). The main advantage of central moments is their invariance to translations of the object, which make it suitable for scene recognition. Paul, Bhattacharya, and Chowdhury (2012b) described a digit recognition system for visually impaired persons using central moments. In Singh, Gupta, and Gupta (2011), an approach for bamboo classification using central moments was proposed. Mertzios (1993) applied scaled normalized central moments for classification and discrimination of industrial objects, in robotic vision applications.

Hu (1962b) proposed a theory of a two-dimensional moment invariant for planar geometric figures. Moments of Hu, or invariant moments, are based on recognition capacities independently of orientation, size and position. These methods are normally used to identify objects due to their descriptive abilities (Flusser, Suk, Boldys, & Zitova, 2015; Licciardi et al., 2012; Yang et al., 2011b). Bessa, Barroso, da Rocha Neto, and de Alexandria (2015) evaluated the use of Hu moments in omnidirectional images with Artificial Neural Networks for mobile robot localization tasks.

Haralick (1979) proposed an approach to represent textures based on second-order statistics with the use of a co-occurrence matrix, called Gray Level Co-occurrence Matrix (GLCM). A co-occurrence matrix describes the amount of combinations of gray levels in an image with a given direction. Texture analysis has been widely applied in fields, such as human robot interaction tasks (Latif, Yusof, Sidek, & Rusli, 2015), medical image analysis (Beura, Majhi, & Dash, 2015), image search (Chu, Hong, Liu, & Chen, 2014), and visual interpretation of remote sensing images (Alves, Clua, & Leta, 2012), among others.

Local Binary Patterns (LBP) is a method for texture description. In this method, each pixel of the image is replaced by a binary value. This value is determined by comparison of a square matrix containing the neighboring pixels, where each pixel is compared with the central. The value obtained for each neighbor is connected and the binary number generated is converted to decimal. The image produced can be split into regions, usually organized in a grid. Finally, the descriptors are extracted from each region individually, and the histogram is computed. The resultant vector is concatenated in a single matrix (Ojala, Pietikainen, & Maenpaa, 2002). LBP is a powerful texture descriptor that is a gray-scale and rotation invariant. Therefore LBP is a suitable feature extractor to use in vision-based localization. Mozos, Mizutani, Kurazume, and Hasegawa (2012) used LBP to categorize areas in indoor environments. Singh, Maurya, and Mittal (2012) combined LBP with SVM for facial expression recognition tasks.

Scale Invariant Feature Transform (SIFT) extracts relevant features of images and maintains them in their descriptor (Lowe, 2004). SIFT is a scaling and rotation invariant. These descriptors create vector-specific information points that can be used to build a training data set. After finding the descriptors, the common points in the two images need to be matched. This procedure can be performed using the kNN or kd-tree. Piccinini, Prati, and Cucchiara (2012) used SIFT to detect and locate duplicate elements in pick-and-place applications.

Speed Up Robust Features (SURF), proposed by Bay, Ess, Tuytelaars, and Van Gool (2008), is a fast and robust method to extract and describe points of interest in images. SURF was partially inspired by SIFT. The authors state that their version extracts points of interest more representative and faster than SIFT. The SURF descriptor, which consists of two principal parts: the detector and the descriptor (Sykora, Kamencay, & Hudec, 2014), uses a determinant of the Hessian matrix to detect feature points (Kang, Choi, & Lim, 2015). SURF is robust to noise and invariant to the rotation, these characteristics can be very relevant in scene recognition. In Niu, Ramana, Wang, and Rodrigues (2014), SURF was applied for indoor localization.

The moments, GLCM and LBP were used for machine learning classifiers to evaluate techniques that would perform better together. SIFT and SURF were evaluated separately. The machine learning techniques used are described in the next section.

4. Overview of machine learning methods

In this section, the six machine learning techniques used in our comparison are defined.

Minimal Learning Machine (MLM) is a machine learning algorithm used for classification and regression. In this method, a geometrical relation between data in the input and output space is considered. This mapping is calculated using a linear model between distance matrices. Minimal Learning Machine algorithm can be separated into two main steps: distance regression and output estimation. Given a test point, the distances from the K reference points are collected and the distances in output space are estimated. The equation to find an estimate to the test point output can be formulated as an optimization problem (de Souza Júnior, Corona, Barreto, Miche, & Lendasse, 2015). The only hyperparameter of MLM is the number of reference points K. MLM can be extended for classification problems representing the S classes in vector form through the codification binary scheme (1-of-S).

The strategy to find the output through the optimization procedure can be computationally "expensive". Therefore, Mesquita, Gomes, and Junior (2015) proposed a fast approach to estimate the output step. An alternative way to compute the estimate for the output $\mathbf{y}$ is based on k-Nearest Neighbors. In this approach, since the distances have been estimated, classes of K, the nearest points of references in the output space $\mathbf{y}$, can be used to estimate the test sample class l. Among the possibilities, the majority vote strategy is adopted, in which the test sample neighbors receive the most frequent value in the K closer classes. In this paper, the MLM net with the approach of the Nearest Neighbors is written using the acronym MLM-NN (MLM-Nearest Neighbors).

The Bayesian classifier is a machine learning method based on Bayes' theorem. With this technique, a sample is classified through the posterior probability using the priori and class-conditional probabilities (Duda, Hart, & Stork, 2000; Theodoridis & Koutroumbas, 2008). In addition, the probability density function (pdf) is estimated by the training data. The pdf can be estimated through parametric methods. The most common rule is based on normal distribution or Gaussian distribution. Mean and covariance matrixes are the only two parameters. Hsieh and Chen (2012) presented a system that automatically recognizes whether the image outside the vehicle is a daytime image or a nighttime image. The detection module and the search module are used to find a system-defined feature region, and the recognition module is used to recognize feature values using a Bayes classifier.

Multi-layer perceptron (MLP) is a combination of Perceptron to solve multi-class problems (Haykin, 2008). Its architecture is composed of neuron layers, such that each layer is fully connected to the next one. MLP has one or more hidden layers, which are formed by hidden neurons. According to Haykin (2008), the hidden neurons intervene between the input and output layers enabling the network to extract high-level statistics. The connection weights in the network measure the degree of correlation between the activity levels of neurons that they connect. Moreover, a training algorithm must be applied to adjust the weights (de Azevedo, Brasil, & ao de Oliveira, 2000; Cortes & Vapnik, 1995; Haykin, 2008; de Sá Medeiros, 2008). The Levenberg–Marquardt algorithm is more effective than the conventional gradient descent algorithms (Liu, 2010). Youssef, Argentieri, and Zarader (2012) used MLP in the localization problem.

Support Vector Machine (SVM) has a well-founded mathematical theory used for classification and regression analysis. Among the advantages of SVM is the induction of a decision hyperplane which can be described in terms of a relatively small quantity of input examples. In other words, sparse solutions are developed. These input patterns are called Support Vectors, in general, they stay near the separation margin. The dual problem that arises in SVM formulation is normally solved by Quadratic programming (QP) (Vapnik, 1998). Another common feature in SVM is the formulation that aims to solve a binary problem. There are SVM formulations for multi-class problems (Crammer, Singer, Cristianini, Shawe-taylor, & Williamson, 2001), however, because of their complexity, a combination of binary classifier outputs have to be used. The approach one-versus-one (Duan & Keerthi, 2005), one-versus-all (Duan & Keerthi, 2005), DAGSVM (Platt, Cristianini, & Shawe-taylor, 2000) and the error correcting code (Dietterich & Bakiri, 1995) are the ones that are most commonly used. The kernel trick is used to create non-linear versions, since the standard is linear. In Li et al. (2016), a scene classification method was proposed using SVM.

Table 5
Specificity(Spe), sensitivity (Sen), positive predictive value (PPV), F-Score (FS), Harmonic means (HM) and Accuracy (Acc) obtained by features extraction and classifiers in the **virtual environment**.

Feature	Classifier	Setup	Spe (%)	Sen (%)	PPV (%)	FS (%)	HM (%)	Acc (%)
Central M.	Bayes	**Normal**	**99.7 ± 0.1**	**96.3 ± 1.1**	**96.5 ± 1.0**	**96.1 ± 1.2**	**97.7 ± 0.7**	**96.3 ± 1.1**
	LSSVM	Linear	87.3 ± 1.2	30.2 ± 2.4	29.7 ± 4.0	23.6 ± 3.3	31.5 ± 4.1	30.2 ± 2.4
		RBF	99.4 ± 0.2	92.6 ± 2.2	93.7 ± 1.8	92.4 ± 2.3	95.4 ± 1.5	92.6 ± 2.2
	MLM	City Block	99.4 ± 0.2	92.1 ± 2.5	92.5 ± 2.5	92.0 ± 2.6	95.2 ± 1.7	92.1 ± 2.5
		Euclidean	**99.6 ± 0.1**	**94.9 ± 1.6**	**95.2 ± 1.7**	**94.8 ± 1.7**	**96.8 ± 1.1**	**94.9 ± 1.6**
		Mahalanobis	99.4 ± 0.2	91.5 ± 2.4	92.2 ± 2.3	91.4 ± 2.5	94.8 ± 1.6	91.5 ± 2.4
	MLM-NN	City Block	99.4 ± 0.2	92.1 ± 2.3	92.5 ± 2.3	92.0 ± 2.4	95.3 ± 1.5	92.1 ± 2.3
		Euclidean	**99.6 ± 0.1**	**94.9 ± 1.6**	**95.2 ± 1.7**	**94.8 ± 1.7**	**96.8 ± 1.1**	**94.9 ± 1.6**
		Mahalanobis	99.4 ± 0.2	91.5 ± 2.4	92.2 ± 2.3	91.4 ± 2.5	94.8 ± 1.6	91.5 ± 2.4
	MLP		99.5 ± 0.2	93.3 ± 2.0	93.3 ± 3.4	92.8 ± 2.7	95.5 ± 2.0	93.3 ± 2.0
	SVM	Linear	96.8 ± 0.5	67.2 ± 3.2	68.0 ± 4.1	63.5 ± 3.9	72.7 ± 3.2	67.2 ± 3.2
		RBF	99.4 ± 0.2	92.3 ± 2.8	93.7 ± 2.2	92.3 ± 2.9	95.2 ± 2.0	92.3 ± 2.8
GLCM	Bayes	Normal	98.5 ± 0.2	82.1 ± 2.5	86.0 ± 2.5	80.5 ± 2.6	86.8 ± 1.9	82.1 ± 2.5
	LSSVM	Linear	98.2 ± 0.3	78.7 ± 3.1	82.1 ± 2.9	75.9 ± 2.9	82.7 ± 2.4	78.7 ± 3.1
		RBF	99.8 ± 0.1	97.9 ± 0.7	98.0 ± 0.6	97.9 ± 0.7	98.8 ± 0.4	97.9 ± 0.7
	MLM	City Block	99.7 ± 0.1	95.8 ± 1.8	96.2 ± 1.8	95.8 ± 1.9	97.6 ± 1.1	95.8 ± 1.8
		Euclidean	99.9 ± 0.1	98.3 ± 1.4	98.4 ± 1.3	98.2 ± 1.5	99.0 ± 0.9	98.3 ± 1.4
		Mahalanobis	**100.0 ± 0.0**	**99.5 ± 0.4**	**99.5 ± 0.4**	**99.5 ± 0.4**	**99.7 ± 0.2**	**99.5 ± 0.4**
	MLM-NN	City Block	99.7 ± 0.1	95.8 ± 1.8	96.2 ± 1.8	95.8 ± 1.9	97.6 ± 1.1	95.8 ± 1.8
		Euclidean	99.9 ± 0.1	98.3 ± 1.4	98.4 ± 1.3	98.2 ± 1.5	99.0 ± 0.9	98.3 ± 1.4
		Mahalanobis	**100.0 ± 0.0**	**99.5 ± 0.4**	**99.5 ± 0.4**	**99.5 ± 0.4**	**99.7 ± 0.2**	**99.5 ± 0.4**
	MLP		99.7 ± 0.3	96.2 ± 3.5	94.8 ± 5.9	95.3 ± 4.8	96.9 ± 3.5	96.2 ± 3.5
	SVM	Linear	99.8 ± 0.1	96.8 ± 1.5	97.2 ± 1.3	96.8 ± 1.5	98.1 ± 0.9	96.8 ± 1.5
		RBF	99.8 ± 0.1	97.1 ± 1.3	97.4 ± 1.2	97.1 ± 1.4	98.3 ± 0.8	97.1 ± 1.3
Hu	Bayes	Normal	95.8 ± 0.3	57.2 ± 2.0	51.0 ± 2.7	51.4 ± 1.3	58.5 ± 1.4	57.2 ± 2.0
	LSSVM	Linear	88.2 ± 0.4	19.9 ± 0.7	9.0 ± 4.9	9.3 ± 1.1	12.1 ± 1.1	19.9 ± 0.7
		RBF	96.6 ± 0.3	65.2 ± 2.2	57.5 ± 1.5	58.4 ± 2.3	66.7 ± 1.8	65.2 ± 2.2
	MLM	City Block	97.9 ± 0.2	76.1 ± 1.5	76.9 ± 1.5	75.8 ± 1.6	83.9 ± 1.3	76.1 ± 1.5
		Euclidean	97.7 ± 0.4	75.0 ± 3.1	76.0 ± 3.0	74.8 ± 2.9	82.8 ± 2.4	75.0 ± 3.1
		Mahalanobis	**98.5 ± 0.2**	**81.8 ± 2.3**	**82.5 ± 2.4**	**81.5 ± 2.5**	**88.2 ± 1.7**	**81.8 ± 2.3**
	MLM-NN	City Block	97.9 ± 0.1	76.1 ± 1.0	77.2 ± 1.0	75.9 ± 0.9	84.0 ± 0.7	76.1 ± 1.0
		Euclidean	97.8 ± 0.4	75.3 ± 3.1	76.2 ± 3.0	75.0 ± 2.9	83.0 ± 2.3	75.3 ± 3.1
		Mahalanobis	**98.5 ± 0.2**	**81.7 ± 2.3**	**82.4 ± 2.5**	**81.4 ± 2.5**	**88.1 ± 1.7**	**81.7 ± 2.3**
	MLP		97.6 ± 0.9	74.1 ± 7.5	74.2 ± 9.6	72.3 ± 8.6	80.1 ± 7.2	74.1 ± 7.5
	SVM	Linear	93.7 ± 0.8	49.6 ± 3.4	43.3 ± 4.3	41.7 ± 4.1	51.7 ± 4.3	49.6 ± 3.4
		RBF	97.0 ± 0.3	68.5 ± 2.2	69.5 ± 5.4	63.5 ± 1.9	72.3 ± 1.4	68.5 ± 2.2
LBP	Bayes	Normal	100.0 ± 0.0	99.9 ± 0.3	99.9 ± 0.3	99.9 ± 0.3	99.9 ± 0.2	99.9 ± 0.3
	LSSVM	Linear	99.8 ± 0.1	96.9 ± 1.3	97.3 ± 1.2	96.9 ± 1.4	98.2 ± 0.8	96.9 ± 1.3
		RBF	100.0 ± 0.0	99.5 ± 0.6	99.5 ± 0.6	99.5 ± 0.6	99.7 ± 0.3	99.5 ± 0.6
	MLM	City Block	100.0 ± 0.0	99.5 ± 0.4	99.6 ± 0.4	99.5 ± 0.5	99.7 ± 0.3	99.5 ± 0.4
		Euclidean	100.0 ± 0.0	99.7 ± 0.4	99.7 ± 0.3	99.7 ± 0.4	99.8 ± 0.2	99.7 ± 0.4
		Mahalanobis	**100.0 ± 0.0**	**100.0 ± 0.0**	**100.0 ± 0.0**	**100.0 ± 0.0**	**100.0 ± 0.0**	**100.0 ± 0.0**
	MLM-NN	City Block	100.0 ± 0.0	99.5 ± 0.4	99.6 ± 0.4	99.5 ± 0.5	99.7 ± 0.3	99.5 ± 0.4
		Euclidean	100.0 ± 0.0	99.7 ± 0.4	99.7 ± 0.3	99.7 ± 0.4	99.8 ± 0.2	99.7 ± 0.4
		Mahalanobis	**100.0 ± 0.0**	**100.0 ± 0.0**	**100.0 ± 0.0**	**100.0 ± 0.0**	**100.0 ± 0.0**	**100.0 ± 0.0**
	MLP		100.0 ± 0.0	99.8 ± 0.4	99.8 ± 0.4	99.8 ± 0.5	99.9 ± 0.3	99.8 ± 0.4
	SVM	Linear	100.0 ± 0.1	99.3 ± 0.9	99.4 ± 0.8	99.3 ± 0.9	99.6 ± 0.5	99.3 ± 0.9
		RBF	100.0 ± 0.0	99.6 ± 0.5	99.6 ± 0.4	99.6 ± 0.5	99.8 ± 0.3	99.6 ± 0.5
Statistics M.	Bayes	**Normal**	**99.9 ± 0.1**	**98.4 ± 0.7**	**98.6 ± 0.6**	**98.4 ± 0.7**	**99.1 ± 0.4**	**98.4 ± 0.7**
	LSSVM	Linear	89.4 ± 0.7	34.7 ± 1.8	34.0 ± 4.7	27.1 ± 2.4	35.9 ± 2.7	34.7 ± 1.8
		RBF	98.9 ± 0.2	86.5 ± 2.3	89.7 ± 1.9	85.6 ± 2.5	90.6 ± 1.8	86.5 ± 2.3
	MLM	City Block	98.9 ± 0.2	86.7 ± 1.7	87.6 ± 2.0	86.6 ± 1.8	91.8 ± 1.4	86.7 ± 1.7
		Euclidean	99.2 ± 0.1	90.1 ± 1.4	90.9 ± 1.4	90.0 ± 1.4	94.0 ± 0.9	90.1 ± 1.4
		Mahalanobis	**99.7 ± 0.1**	**95.8 ± 1.6**	**96.2 ± 1.6**	**95.8 ± 1.6**	**97.5 ± 1.0**	**95.8 ± 1.6**
	MLM-NN	City Block	98.9 ± 0.2	86.9 ± 2.0	87.7 ± 2.2	86.8 ± 2.0	91.9 ± 1.5	86.9 ± 2.0
		Euclidean	99.2 ± 0.1	90.1 ± 1.3	90.9 ± 1.4	90.0 ± 1.3	94.0 ± 0.8	90.1 ± 1.3
		Mahalanobis	**99.7 ± 0.1**	**95.9 ± 1.5**	**96.3 ± 1.4**	**95.9 ± 1.5**	**97.6 ± 0.9**	**95.9 ± 1.5**
	MLP		99.0 ± 0.3	87.2 ± 3.0	86.6 ± 4.8	86.3 ± 4.1	91.1 ± 3.2	87.2 ± 3.0
	SVM	Linear	95.5 ± 1.0	59.4 ± 6.0	55.0 ± 6.7	51.7 ± 7.4	62.1 ± 7.4	59.4 ± 6.0
		RBF	99.3 ± 0.2	91.4 ± 2.6	93.0 ± 1.9	91.2 ± 2.6	94.6 ± 1.7	91.4 ± 2.6
	SIFT		**99.9 ± 0.1**	**98.8 ± 0.9**	**99.0 ± 0.8**	**98.8 ± 0.9**	**99.3 ± 0.5**	**98.8 ± 0.9**
	SURF		**99.3 ± 0.2**	**90.7 ± 2.0**	**91.7 ± 1.6**	**90.3 ± 2.2**	**94.0 ± 1.6**	**90.7 ± 2.0**

The Least Squares Support Vector Machine (LSSVM) was proposed by Suykens and Vandewalle (1999). LSSVM classifiers are also able to solve classification problems and function approximations. LSSVM is a viable alternative for the standard SVM formulation, due to the use of a system of linear equations, Karush-Kuhn-Tucker (KKT), in the training phase. In contrast, the quadratic programing used in SVM has a high computational cost. Detailed information is found in Suykens and Vandewalle (1999) and Tsujinishi and Abe (2003). LSSVM was applied in color image segmentation by Yang, Wang, Wang, and Zhang (2012).

Table 6
Specificity(Spe), sensitivity (Sen), positive predictive value (PPV), F-Score (FS), Harmonic means (HM) and Accuracy (Acc) obtained by features extraction and classifiers in the **real environment**.

Feature	Classifier	Setup	Spe (%)	Sen (%)	PPV (%)	FS (%)	HM (%)	Acc (%)
Central M.	Bayes	Normal	99.3 ± 0.2	91.4 ± 2.1	92.2 ± 1.8	91.4 ± 2.1	94.9 ± 1.3	91.4 ± 2.1
	LSSVM	Linear	89.6 ± 0.7	34.5 ± 1.7	26.4 ± 3.3	23.7 ± 1.5	32.2 ± 2.0	34.5 ± 1.7
		RBF	99.5 ± 0.2	93.2 ± 2.4	94.3 ± 1.7	93.2 ± 2.4	95.9 ± 1.6	93.2 ± 2.4
	MLM	City Block	98.9 ± 0.3	86.1 ± 2.7	87.0 ± 2.6	85.8 ± 2.8	91.2 ± 2.0	86.1 ± 2.7
		Euclidean	**99.6 ± 0.1**	**94.8 ± 1.1**	**95.2 ± 1.2**	**94.8 ± 1.2**	**97.0 ± 0.7**	**94.8 ± 1.1**
		Mahalanobis	**99.6 ± 0.1**	**94.3 ± 1.9**	**94.8 ± 1.9**	**94.2 ± 2.0**	**96.6 ± 1.2**	**94.3 ± 1.9**
	MLM-NN	City Block	98.9 ± 0.3	86.3 ± 2.7	87.2 ± 2.7	86.0 ± 2.9	91.4 ± 2.0	86.3 ± 2.7
		Euclidean	**99.6 ± 0.1**	**94.8 ± 1.1**	**95.2 ± 1.2**	**94.8 ± 1.2**	**97.0 ± 0.7**	**94.8 ± 1.1**
		Mahalanobis	**99.6 ± 0.1**	**94.3 ± 1.9**	**94.8 ± 1.9**	**94.2 ± 2.0**	**96.6 ± 1.2**	**94.3 ± 1.9**
	MLP		99.0 ± 0.6	88.4 ± 6.4	85.5 ± 10.4	86.3 ± 8.8	90.7 ± 6.8	88.4 ± 6.4
	SVM	Linear	97.6 ± 0.6	73.7 ± 5.1	79.7 ± 5.1	72.1 ± 5.8	80.2 ± 4.9	73.7 ± 5.1
		RBF	99.4 ± 0.2	92.1 ± 2.7	93.5 ± 2.0	92.1 ± 2.7	95.2 ± 1.8	92.1 ± 2.7
GLCM	Bayes	Normal	97.3 ± 0.3	71.5 ± 2.6	74.0 ± 4.9	69.5 ± 3.2	78.7 ± 2.6	71.5 ± 2.6
	LSSVM	Linear	94.0 ± 0.6	50.9 ± 2.6	51.5 ± 3.8	44.4 ± 3.3	55.2 ± 3.2	50.9 ± 2.6
		RBF	98.9 ± 0.3	86.1 ± 2.9	88.4 ± 2.5	86.0 ± 2.9	91.2 ± 2.1	86.1 ± 2.9
	MLM	City Block	98.3 ± 0.3	80.5 ± 2.5	81.7 ± 2.4	80.3 ± 2.5	87.6 ± 1.7	80.5 ± 2.5
		Euclidean	98.8 ± 0.2	85.1 ± 2.3	86.7 ± 2.3	85.1 ± 2.3	90.8 ± 1.5	85.1 ± 2.3
		Mahalanobis	**99.4 ± 0.2**	**91.7 ± 2.6**	**92.5 ± 2.3**	**91.7 ± 2.6**	**95.1 ± 1.6**	**91.7 ± 2.6**
	MLM-NN	City Block	98.3 ± 0.3	80.6 ± 2.5	81.8 ± 2.4	80.4 ± 2.6	87.7 ± 1.8	80.6 ± 2.5
		Euclidean	98.8 ± 0.2	85.1 ± 2.3	86.7 ± 2.3	85.1 ± 2.3	90.8 ± 1.5	85.1 ± 2.3
		Mahalanobis	**99.4 ± 0.2**	**91.7 ± 2.6**	**92.5 ± 2.3**	**91.7 ± 2.6**	**95.1 ± 1.6**	**91.7 ± 2.6**
	MLP		98.5 ± 0.7	82.9 ± 6.3	81.9 ± 9.2	81.6 ± 7.9	88.0 ± 6.0	82.9 ± 6.3
	SVM	Linear	97.4 ± 0.4	72.2 ± 3.4	76.0 ± 5.1	69.7 ± 4.2	77.7 ± 3.8	72.2 ± 3.4
		RBF	98.8 ± 0.2	85.5 ± 1.7	88.3 ± 1.4	85.7 ± 1.7	91.0 ± 1.3	85.5 ± 1.7
Hu	Bayes	Normal	99.0 ± 0.2	87.5 ± 2.3	88.6 ± 2.4	87.1 ± 2.3	91.9 ± 1.5	87.5 ± 2.3
	LSSVM	Linear	91.9 ± 0.6	41.2 ± 2.1	40.3 ± 6.4	31.4 ± 2.4	41.3 ± 2.6	41.2 ± 2.1
		RBF	98.8 ± 0.2	85.7 ± 2.0	89.1 ± 1.1	85.7 ± 1.9	90.9 ± 1.5	85.7 ± 2.0
	MLM	City Block	97.7 ± 0.5	74.8 ± 3.7	76.0 ± 4.0	74.6 ± 3.9	83.6 ± 2.8	74.8 ± 3.7
		Euclidean	99.2 ± 0.2	89.7 ± 2.7	90.5 ± 2.6	89.5 ± 2.9	93.8 ± 1.9	89.7 ± 2.7
		Mahalanobis	**99.2 ± 0.2**	**90.4 ± 2.6**	**91.1 ± 2.3**	**90.4 ± 2.6**	**94.3 ± 1.6**	**90.4 ± 2.6**
	MLM-NN	City Block	97.7 ± 0.4	74.9 ± 3.6	76.0 ± 3.9	74.7 ± 3.8	83.7 ± 2.8	74.9 ± 3.6
		Euclidean	99.2 ± 0.2	89.7 ± 2.7	90.5 ± 2.6	89.5 ± 2.9	93.8 ± 1.9	89.7 ± 2.7
		Mahalanobis	**99.2 ± 0.2**	**90.4 ± 2.6**	**91.1 ± 2.3**	**90.4 ± 2.6**	**94.3 ± 1.6**	**90.4 ± 2.6**
	MLP		98.6 ± 0.4	83.6 ± 4.5	81.9 ± 7.1	81.9 ± 5.9	88.1 ± 4.5	83.6 ± 4.5
	SVM	Linear	95.0 ± 0.6	55.6 ± 3.2	61.9 ± 6.2	49.9 ± 4.1	59.8 ± 4.0	55.6 ± 3.2
		RBF	98.8 ± 0.2	85.1 ± 2.7	88.0 ± 2.0	85.3 ± 2.6	90.8 ± 1.8	85.1 ± 2.7
LBP	Bayes	Normal	99.3 ± 0.1	90.6 ± 1.7	91.2 ± 1.5	90.5 ± 1.7	94.3 ± 1.1	90.6 ± 1.7
	LSSVM	Linear	97.7 ± 0.3	74.3 ± 3.1	78.3 ± 2.8	71.9 ± 3.3	79.6 ± 2.7	74.3 ± 3.1
		RBF	99.6 ± 0.1	95.3 ± 1.6	95.8 ± 1.3	95.2 ± 1.6	97.2 ± 1.0	95.3 ± 1.6
	MLM	City Block	99.6 ± 0.1	94.2 ± 0.8	94.7 ± 0.9	94.2 ± 0.8	96.6 ± 0.5	94.2 ± 0.8
		Euclidean	99.6 ± 0.1	95.1 ± 1.0	95.4 ± 0.9	95.0 ± 1.0	97.1 ± 0.6	95.1 ± 1.0
		Mahalanobis	**99.8 ± 0.1**	**96.7 ± 1.4**	**96.9 ± 1.3**	**96.6 ± 1.4**	**98.1 ± 0.8**	**96.7 ± 1.4**
	MLM-NN	City Block	99.6 ± 0.1	94.2 ± 0.8	94.7 ± 0.9	94.2 ± 0.8	96.6 ± 0.5	94.2 ± 0.8
		Euclidean	99.6 ± 0.1	95.1 ± 1.0	95.4 ± 0.9	95.0 ± 1.0	97.1 ± 0.6	95.1 ± 1.0
		Mahalanobis	**99.8 ± 0.1**	**96.7 ± 1.4**	**96.9 ± 1.3**	**96.6 ± 1.4**	**98.1 ± 0.8**	**96.7 ± 1.4**
	MLP		99.5 ± 0.2	93.9 ± 2.8	93.4 ± 4.5	93.3 ± 3.7	95.8 ± 2.8	93.9 ± 2.8
	SVM	Linear	99.3 ± 0.2	91.3 ± 2.9	92.9 ± 2.4	91.5 ± 2.8	94.8 ± 1.8	91.3 ± 2.9
		RBF	99.6 ± 0.1	94.5 ± 1.3	95.2 ± 1.1	94.5 ± 1.3	96.8 ± 0.8	94.5 ± 1.3
Statistics M.	Bayes	**Normal**	**99.7 ± 0.1**	**96.5 ± 1.7**	**96.8 ± 1.6**	**96.4 ± 1.7**	**97.9 ± 1.0**	**96.5 ± 1.7**
	LSSVM	Linear	90.1 ± 0.6	36.6 ± 1.7	31.4 ± 4.1	26.2 ± 2.3	35.8 ± 2.5	36.6 ± 1.7
		RBF	99.4 ± 0.2	91.6 ± 2.5	92.9 ± 2.0	91.4 ± 2.5	94.8 ± 1.6	91.6 ± 2.5
	MLM	City Block	98.7 ± 0.3	83.9 ± 2.8	84.8 ± 2.6	83.7 ± 2.9	89.8 ± 2.0	83.9 ± 2.8
		Euclidean	99.3 ± 0.2	91.1 ± 2.0	91.8 ± 2.0	91.0 ± 2.0	94.6 ± 1.2	91.1 ± 2.0
		Mahalanobis	**99.6 ± 0.1**	**94.3 ± 1.2**	**94.8 ± 1.2**	**94.2 ± 1.2**	**96.6 ± 0.7**	**94.3 ± 1.2**
	MLM-NN	City Block	98.7 ± 0.3	83.9 ± 2.8	84.7 ± 2.6	83.6 ± 2.9	89.8 ± 2.0	83.9 ± 2.8
		Euclidean	99.3 ± 0.2	91.1 ± 2.0	91.8 ± 2.0	91.0 ± 2.0	94.6 ± 1.2	91.1 ± 2.0
		Mahalanobis	**99.6 ± 0.1**	**94.3 ± 1.2**	**94.8 ± 1.2**	**94.2 ± 1.2**	**96.6 ± 0.7**	**94.3 ± 1.2**
	MLP		98.5 ± 0.4	82.5 ± 3.8	78.3 ± 7.2	79.4 ± 5.5	86.0 ± 4.4	82.5 ± 3.8
	SVM	Linear	97.5 ± 0.4	72.1 ± 3.1	74.8 ± 3.1	70.1 ± 3.3	77.4 ± 2.8	72.1 ± 3.1
		RBF	99.2 ± 0.2	90.1 ± 2.8	91.9 ± 2.6	90.2 ± 2.9	94.0 ± 1.8	90.1 ± 2.8
	SIFT		**95.7 ± 0.1**	**61.0 ± 0.6**	**62.4 ± 3.6**	**59.3 ± 2.7**	**71.2 ± 2.9**	**61.0 ± 0.6**
	SURF		**92.8 ± 0.8**	**47.3 ± 3.3**	**49.9 ± 2.1**	**46.2 ± 3.8**	**59.1 ± 4.5**	**47.3 ± 3.3**

5. Methodology

In this section, we explain the methodology of the proposed method, the robot, the topological map of the environment and the dataset generated by the features extraction and machine learning techniques.

Table 7
Accuracy (Acc), training time, testing time and feature extraction time for all features extraction in virtual and real environments obtained by the best classifiers.

Virtual environment				
Classifier	Acc(%)	Training Time (s)	Testing Time (us)	Extraction Time (s)
Central moments				
Bayes (Normal)	96.3 ± 1.1	0.003 ± 0.0	68.6 ± 18.7	0.067 ± 0.02
MLM (Euclidean)	94.9 ± 1.6	0.068 ± 0.0	28327.6 ± 1274.2	
MLM-NN (Euclidean)	94.9 ± 1.6	0.068 ± 0.0	120.2 ± 1.8	
GLCM				
MLM (Mahalanobis)	99.5 ± 0.4	0.152 ± 0.0	16186.1 ± 325.4	0.115 ± 0.02
MLM-NN (Mahalanobis)	99.5 ± 0.4	0.139 ± 0.0	174.1 ± 2.8	
Hu				
MLM (Mahalanobis)	81.8 ± 2.3	0.127 ± 0.0	15904.3 ± 187.3	0.107 ± 0.02
MLM-NN (Mahalanobis)	81.7 ± 2.3	0.123 ± 0.0	152.2 ± 7.1	
LBP				
MLM (Mahalanobis)	100.0 ± 0.0	0.244 ± 0.1	16633.6 ± 412.3	0.202 ± 0.02
MLM-NN (Mahalanobis)	100.0 ± 0.0	0.216 ± 0.0	309.8 ± 16.4	
Statistical moments				
Bayes (Normal)	98.4 ± 0.7	0.645 ± 2.0	1119.6 ± 3439.9	0.040 ± 0.02
MLM (Euclidean)	95.8 ± 1.6	0.138 ± 0.0	15957.0 ± 258.5	
MLM-NN (Euclidean)	95.9 ± 1.5	0.122 ± 0.0	158.0 ± 7.0	
SIFT	98.8 ± 0.9	4.465 ± 0.2	559628.4 ± 168723.9	0.377 ± 0.03
SURF	90.7 ± 2.0	1.931 ± 2.1	216752.0 ± 344680.1	0.233 ± 0.02
Real environment				
Classifier	Acc(%)	Training Time (s)	Testing Time (us)	Extraction Time (s)
Central moments				
MLM (Euclidean	94.8 ± 1.1	0.072 ± 0.0	63868.8 ± 2571.1	2.302 ± 0.59
MLM-NN (Euclidean)	94.8 ± 1.1	0.070 ± 0.0	119.7 ± 5.0	
MLM (Mahalanobis)	94.3 ± 1.9	0.196 ± 0.1	34095.6 ± 323.0	
MLM-NN (Mahalanobis)	94.3 ± 1.9	0.129 ± 0.0	136.5 ± 2.7	
GLCM				
MLM (Mahalanobis)	91.7 ± 2.6	0.244 ± 0.1	34508.2 ± 174.7	2.637 ± 0.59
MLM-NN (Mahalanobis)	91.7 ± 2.6	0.209 ± 0.0	274.7 ± 5.5	
Hu				
MLM (Mahalanobis)	90.4 ± 2.6	0.136 ± 0.0	35298.5 ± 757.8	2.469 ± 0.59
MLM-NN (Mahalanobis)	90.4 ± 2.6	0.133 ± 0.0	160.3 ± 15.2	
LBP				
MLM (Mahalanobis)	96.7 ± 1.4	0.835 ± 0.1	35339.9 ± 580.1	5.237 ± 0.59
MLM-NN (Mahalanobis)	96.7 ± 1.4	0.760 ± 0.0	1207.9 ± 23.2	
Statistical moments				
Bayes (Normal)	96.5 ± 1.7	0.004 ± 0.0	59.5 ± 70.6	2.241 ± 0.59
MLM (Mahalanobis)	94.3 ± 1.2	0.175 ± 0.1	34266.9 ± 141.2	
MLM-NN (Mahalanobis)	94.3 ± 1.2	0.145 ± 0.0	165.9 ± 15.1	
SIFT	61.0 ± 0.6	189.134 ± 3.0	36557603.0 ± 3044694.6	10.353 ± 0.35
SURF	47.3 ± 3.3	30.242 ± 0.4	2057985.3 ± 67369.9	6.919 ± 0.26

5.1. Proposed method for localization via classification with a reject option

Reject option can be used to increase the reliability of the classifier in some decision systems. In this approach, an element that is not considered sufficiently reliable is automatically rejected. The element is then directed to a human expert or to another classifier (Gamelas Sousa et al., 2015). In this work, we present a different approach of reject option adapted to mobile robot localization using a topological map with omnidirectional images. Consider, for example, a situation represented by Fig. 2 in which the robot is in the place corresponding to class 1 (node 3) and receives a command to move to class 6 (node 2). Arriving at the destination, the classifier predicts that there is a higher probability of the place being class 12 (node 6) and a second higher probability to be the class 6.

More formally, we define the topological map as graph $G = (V, E)$, where V is a set of nodes (which contains the classes) and E is a set of edges (paths through the classes). Given a test sample $\mathbf{x}$ extracted from an image captured by an omnidirectional camera, one can use this extractor to identify the node of the robot's position. The result from each classifier using these attributes is a sorted sequence $C = (c_1, c_2, \ldots, c_l)$, wherein l is the number of classes. In the sequence C, c_1 and c_2 are the first and second classes more likely to be $\mathbf{x}$. When the robot receives a command to move to node n_1 and the first class c_1 estimated by the classifier is a class of node n_2, where n_1 and n_2 are not adjacent, then the second class (c_2) is assigned to $\mathbf{x}$. Otherwise, the choice for the first class is maintained. This approach is called localization with reject option in this paper. Results show that localization with a reject option increased the accuracy of all classifiers.

5.2. Description of the information flow to compare the methods

During navigation, the robot uses the vision-based localization system to locate itself. The system begins to work with the capture of images. An omnidirectional image is obtained through the Dot, a lens that can shoot 360° pictures. Once obtained the digital image, is analyzed by the system, which begins with feature extraction. In this paper, Central Moments, GLCM, Hu moments, LBP and Statistics Moments are evaluated. The feature vectors are presented to a classifier to perform the recognition of the environment. In this step, six machine learning techniques are

Table 8
Accuracy (Acc), F-Score (FS) and Harmonic means (HM) for mean case of the classifiers for each feature extraction technique in virtual and real environments, respectively.

Virtual environment							Real environment					
Class	Central moment											
	Bayes (Normal)			MLM-NN (Euclidean)			MLM (Euclidean)			MLM-NN (Mahalanobis)		
	Acc(%)	FS(%)	HM(%)	Acc(%)	FS(%)	HM(%)	Acc(%)	FS(%)	HM(%)	Acc(%)	FS(%)	HM(%)
1	99.9	100	99.4	100	99.7	99	99.7	98.7	99.9	99.7	98.6	99.9
2	99.7	99.9	99.3	100	99.8	100	100	99.9	99.9	100	99.9	99.6
3	96	100	100	100	99	100	87	99	100	93	99	97
4	97	97	100	100	100	97	84	95	83	84	98	76
5	100	87	99	100	93	67	100	100	99	96	99	95
6	99.1	100	90.6	100	96.4	84.9	96.3	84.8	99.1	96.3	83.9	99.1
7	96.4	98.2	92.1	100	98.3	100	100	99.1	99.1	100	99.1	95.5
8	97.9	96.3	100	98.1	96.2	99.5	88.3	97.6	95	90.7	97.6	93.4
9	97.5	98.4	100	99.5	100	98.4	89.2	95.1	83.3	87.6	95.7	84
10	99.5	90.5	92.2	100	83.6	73.8	100	98.1	99.5	96.5	97.1	95.9
11	98.4	100	82.4	98.9	99.9	81.7	97.2	93.3	98.9	97.2	94.4	98.9
12	99.9	99.9	99.7	100	99.9	100	99.5	96.7	100	99.5	96.7	99.8
13	96	100	100	100	99	100	87	99	100	93	99	97
14	97	97	100	100	100	97	84	95	83	84	98	76
15	100	87	99	100	93	67	100	100	99	96	99	95
Total	96.27	96.15	97.74	94.93	94.78	96.81	94.8	94.77	96.96	94.27	94.17	96.59
	GLCM											
	MLM (Mahalanobis)			MLM-NN (Mahalanobis)			MLM (Mahalanobis)			MLM-NN (Mahalanobis)		
Class	Acc(%)	FS(%)	HM(%)	Acc(%)	FS(%)	HM(%)	Acc(%)	FS(%)	HM(%)	Acc(%)	FS(%)	HM(%)
1	100	100	100	100	100	100	99.2	99.5	99.8	99.2	99.5	99.8
2	99.8	100	100	99.8	100	100	98.9	98.8	100	98.9	98.8	100
3	100	100	100	100	100	100	89	96	99	89	96	99
4	100	100	100	100	100	100	96	84	79	96	84	79
5	100	97	100	100	97	100	100	90	94	100	90	94
6	100	100	100	100	100	100	90.6	94.1	98.1	90.6	94.1	98.1
7	97.3	100	100	97.3	100	100	87.5	86.9	100	87.5	86.9	100
8	100	100	100	100	100	100	84.4	95.9	99.5	84.4	95.9	99.5
9	97.6	100	100	97.6	100	100	96.5	85.7	78.4	96.5	85.7	78.4
10	100	98.4	100	100	98.4	100	99.5	91.7	94.4	99.5	91.7	94.4
11	100	100	98.9	100	100	98.9	90.5	93	99.4	90.5	93	99.4
12	99.9	98.4	100	99.9	98.4	100	95	92.3	99.5	95	92.3	99.5
13	100	100	100	100	100	100	89	96	99	89	96	99
14	100	100	100	100	100	100	96	84	79	96	84	79
15	100	97	100	100	97	100	100	90	94	100	90	94
Total	99.47	99.47	99.7	99.47	99.47	99.7	91.73	91.75	95.12	91.73	91.75	95.12
	Hu											
	MLM (Mahalanobis)			MLM-NN (Mahalanobis)			MLM (Mahalanobis)			MLM-NN (Mahalanobis)		
Class	Acc(%)	FS(%)	HM(%)	Acc(%)	FS(%)	HM(%)	Acc(%)	FS(%)	HM(%)	Acc(%)	FS(%)	HM(%)
1	98.8	96.9	98	98.8	96.9	98	99.1	99.2	99.8	99.1	99.2	99.8
2	99.8	98.7	100	99.8	98.7	100	98.9	99.5	98.8	98.9	99.5	98.8
3	73	100	92	73	100	92	85	94	94	85	94	94
4	91	64	53	91	63	53	88	92	90	88	92	90
5	100	93	71	100	93	71	98	84	93	98	84	93
6	84.6	64.4	74.5	84.6	64.4	74.5	90.1	90.6	98.2	90.1	90.6	98.2
7	98.1	86.4	100	98.1	86.4	100	85.4	94.5	87.4	85.4	94.5	87.4
8	71.2	95.3	94.3	71.2	95.3	94.3	83	92.2	91.8	83	92.2	91.8
9	89.5	60.1	55.9	89.5	59.5	55.6	92.5	92.2	90	92.5	92.2	90
10	95.8	93.1	72.1	95.8	93.1	72.1	97.1	83.2	94.3	97.1	83.2	94.3
11	84.6	76.3	77.9	84.6	76.3	77.9	94.6	91.9	98.3	94.6	91.9	98.3
12	97.8	92.9	100	97.8	92.9	100	89.3	91.9	97.3	89.3	91.9	97.3
13	73	100	92	73	100	92	85	94	94	85	94	94
14	91	64	53	91	63	53	88	92	90	88	92	90
15	100	93	71	100	93	71	98	84	93	98	84	93
Total	81.8	81.5	88.17	81.73	81.44	88.12	90.4	90.36	94.34	90.4	90.36	94.34
	LBP											
	MLM (Mahalanobis)			MLM-NN (Mahalanobis)			MLM (Mahalanobis)			MLM-NN (Mahalanobis)		
Class	Acc(%)	FS(%)	HM(%)	Acc(%)	FS(%)	HM(%)	Acc(%)	FS(%)	HM(%)	Acc(%)	FS(%)	HM(%)
1	100	100	100	100	100	100	99.6	99.6	99.9	99.6	99.6	99.9
2	100	100	100	100	100	100	100	99.3	99.9	100	99.3	99.9
3	100	100	100	100	100	100	93	100	100	93	100	100
4	100	100	100	100	100	100	99	95	92	99	95	92
5	100	100	100	100	100	100	100	99	100	100	99	100
6	100	100	100	100	100	100	94.5	94.3	98.2	94.5	94.3	98.2
7	100	100	100	100	100	100	100	91.5	99.1	100	91.5	99.1

(*continued on next page*)

Table 8 (*continued*)

8	100	100	100	100	100	100	92.9	100	98.6	92.9	100	98.6
9	100	100	100	100	100	100	98.5	95	92.8	98.5	95	92.8
10	100	100	100	100	100	100	100	99.5	98.6	100	99.5	98.6
11	100	100	100	100	100	100	96	94.4	99.9	96	94.4	99.9
12	100	100	100	100	100	100	99.5	95.4	98.9	99.5	95.4	98.9
13	100	100	100	100	100	100	93	100	100	93	100	100
14	100	100	100	100	100	100	99	95	92	99	95	92
15	100	100	100	100	100	100	100	99	100	100	99	100
Total	100	100	100	100	100	100	96.67	96.64	98.09	96.67	96.64	98.09
	Statiscal Moment											
	Bayes (Normal)			MLM-NN (Mahalanobis)			Bayes (Normal)			MLM-NN (Mahalanobis)		
Class	Acc(%)	FS(%)	HM(%)	Acc(%)	FS(%)	HM(%)	Acc(%)	FS(%)	HM(%)	Acc(%)	FS(%)	HM(%)
1	99.9	100	100	99.8	100	99.7	100	99.5	99.9	99.5	99.3	99.7
2	100	99.6	99.7	99.8	99.9	99.6	99.6	99.1	100	99.5	99.8	99.8
3	100	100	100	100	100	100	91	99	100	89	100	100
4	99	100	100	95	100	100	99	93	92	94	89	84
5	100	94	100	86	96	88	100	98	99	97	98	96
6	99.1	100	100	98.1	100	96.3	100	93.8	99.1	93.4	92	96.4
7	100	95.5	96.4	98.2	99.1	94.3	95	89.7	100	94.7	97.9	98.2
8	100	97.2	100	100	100	100	90.9	99.5	98.1	85.4	100	98.6
9	96.3	100	100	89.4	100	100	98.5	93.3	94.3	92.6	87.4	88.3
10	99.5	96.8	100	87.1	92.4	91	98.6	98.9	99.5	98.4	97	97.9
11	95.6	100	97.3	95.6	100	98.3	91	98.7	100	93.9	94.5	98.7
12	97.8	99.8	99.9	96.4	97.3	97.6	99.8	99.6	96.7	99.2	95.6	98.8
13	100	100	100	100	100	100	91	99	100	89	100	100
14	99	100	100	95	100	100	99	93	92	94	89	84
15	100	94	100	86	96	88	100	98	99	97	98	96
Total	98.4	98.38	99.08	95.93	95.91	97.62	96.47	96.41	97.93	94.27	94.25	96.64

used in the experiments. Both SIFT and SURF were evaluated separately. Fig. 3 shows the information flowchart.

5.3. Test application

We used a small mobile robot adapted to locomotion in a home environment, see Fig. 4c. It consisted of a metal platform equipped with engines, logic boards, batteries, and a system of interconnected gears with two pairs of wheels. The robot has its own software that communicates with a microcomputer controlled by telemetry. A camera along with the Dot, a lens that shoots 360° images was used.

The robot navigates in an indoor environment, in this case an apartment. This environment was chosen on account of the existence of features which help the recognition and navigation of the robot. In the topological map, we presented the nodes numbered 1 to 6. We took pictures of the strategic points corresponding to classes numbered 1–15. The edges are the possible paths of the robot during navigation. Fig. 4 shows the detailed diagram of the real environment.

5.4. Dataset description

Our topological navigation vision-based system was evaluated, initially, with images from a virtual environment. We took 50 distinctive images from each class, but with similar information from the point of view of the same node in the map. Similarly, we took 50 images from each class in the real environment. This procedure was necessary in order to ensure correct performance of the navigation system. In this way, possible situations in which the robot is near the node but not actually there, are predicted. Fig. 5b and a show the place corresponding to class 15 (node 5) from both real and virtual environments, respectively. The virtual and real datasets used are available at LAPISCO website.

The five feature extraction techniques were applied in all images obtained in the acquisition phase. Table 3 describes the number of attributes generated by each technique. Subsequently, these samples were classified by Bayes, LSSVM, SVM, MLM, MLM-NN and MLP.

5.5. Navigation tests

We conducted ten experiments using ten different routes in real environments. Table 4 shows the commands used to move the robot, as well, the start and end locations.

Fig. 6 exemplifies the route 7 of Table 2. In this route, the robot begins at node 1 (class 8) and receives two commands to go straight ahead. After that, it turns to the left and receives again two commands to go straight ahead and reaches node 6 (class 12).

6. Results

In this section, we present the results achieved by the machine learning methods on ten data sets generated by feature extraction techniques. Both SIFT and SURF were evaluated separately on images from real and virtual environments.

All data sets were equally preprocessed. The patterns were partitioned randomly in two groups, four fifths for training and the remainder for test, in each of the ten iterations. The training set was then normalized (zero-mean and unit variance) and the test sets were also normalized using the same normalization measures as the training set. The proportions of the classes were kept balanced in both training and test sets.

The hyper-parameters for the SVM, LSSVM and the MLP were chosen using 10-fold cross-validation. SVM and LSSVM were trained using the SVM toolbox (MATLAB, 2013) and default settings for the hyper-parameters. The grid search was logarithmic between 2^{-2} and 2^{11} for each hyper-parameter. Linear kernel and radial basis function kernels were used. MLP was learnt using the Levenberg–Marquardt optimization and a range of hidden units from 1 to 50. The learning of GP was based on the default settings in MATLAB (2013). Bayes classifier was validated using Gaussian Normal probability distribution. MLM and MLM-NN were trained with Euclidean, Manhattan and Mahalanobis distance metrics and

Table 9
Accuracy by route obtained from the feature extraction techniques and classifiers **without reject option**.

Feature	Classifier	Setup	Route 1	Route 2	Route 3	Route 4	Route 5	Route 6	Route 7	Route 8	Route 9	Route 10
Central M.	Bayes	Normal	40.0 ± 51.6	90.0 ± 31.6	40.0 ± 51.6	50.0 ± 52.7	50.0 ± 52.7	70.0 ± 48.3	40.0 ± 51.6	0.0 ± 0.0	90.0 ± 31.6	60.0 ± 51.6
	LSSVM	Linear	0.0 ± 0.0	0.0 ± 0.0	0.0 ± 0.0	0.0 ± 0.0	0.0 ± 0.0	0.0 ± 0.0	0.0 ± 0.0	0.0 ± 0.0	20.0 ± 42.2	0.0 ± 0.0
		RBF	60.0 ± 51.6	40.0 ± 51.6	90.0 ± 31.6	50.0 ± 52.7	50.0 ± 52.7	70.0 ± 48.3	60.0 ± 51.6	50.0 ± 52.7	100.0 ± 0.0	30.0 ± 48.3
	MLM	City Block	20.0 ± 42.2	50.0 ± 52.7	60.0 ± 51.6	10.0 ± 31.6	40.0 ± 51.6	50.0 ± 52.7	20.0 ± 42.2	0.0 ± 0.0	60.0 ± 51.6	40.0 ± 51.6
		Euclidean	70.0 ± 48.3	60.0 ± 51.6	90.0 ± 31.6	70.0 ± 48.3	60.0 ± 51.6	60.0 ± 51.6	80.0 ± 42.2	60.0 ± 51.6	100.0 ± 0.0	70.0 ± 48.3
		Mahalanobis	70.0 ± 48.3	70.0 ± 48.3	80.0 ± 42.2	70.0 ± 48.3	60.0 ± 51.6	60.0 ± 51.6	70.0 ± 48.3	60.0 ± 51.6	80.0 ± 42.2	90.0 ± 31.6
	MLM-NN	City Block	20.0 ± 42.2	50.0 ± 52.7	60.0 ± 51.6	10.0 ± 31.6	40.0 ± 51.6	50.0 ± 52.7	20.0 ± 42.2	0.0 ± 0.0	60.0 ± 51.6	40.0 ± 51.6
		Euclidean	70.0 ± 48.3	60.0 ± 51.6	90.0 ± 31.6	70.0 ± 48.3	60.0 ± 51.6	60.0 ± 51.6	80.0 ± 42.2	60.0 ± 51.6	100.0 ± 0.0	70.0 ± 48.3
		Mahalanobis	70.0 ± 48.3	70.0 ± 48.3	80.0 ± 42.2	70.0 ± 48.3	60.0 ± 51.6	60.0 ± 51.6	70.0 ± 48.3	60.0 ± 51.6	80.0 ± 42.2	90.0 ± 31.6
	MLP		60.0 ± 51.6	50.0 ± 52.7	50.0 ± 52.7	60.0 ± 51.6	50.0 ± 52.7	50.0 ± 52.7	40.0 ± 51.6	60.0 ± 51.6	60.0 ± 51.6	50.0 ± 52.7
	SVM	Linear	0.0 ± 0.0	40.0 ± 51.6	80.0 ± 42.2	20.0 ± 42.2	0.0 ± 0.0	30.0 ± 48.3	20.0 ± 42.2	10.0 ± 31.6	30.0 ± 48.3	10.0 ± 31.6
		RBF	50.0 ± 52.7	50.0 ± 52.7	80.0 ± 42.2	60.0 ± 51.6	70.0 ± 48.3	70.0 ± 48.3	50.0 ± 52.7	40.0 ± 51.6	90.0 ± 31.6	40.0 ± 51.6
GLCM	Bayes	Normal	20.0 ± 42.2	50.0 ± 52.7	20.0 ± 42.2	20.0 ± 42.2	10.0 ± 31.6	30.0 ± 48.3	0.0 ± 0.0	0.0 ± 0.0	0.0 ± 0.0	0.0 ± 0.0
	LSSVM	Linear	0.0 ± 0.0	0.0 ± 0.0	0.0 ± 0.0	0.0 ± 0.0	0.0 ± 0.0	0.0 ± 0.0	0.0 ± 0.0	0.0 ± 0.0	0.0 ± 0.0	0.0 ± 0.0
		RBF	30.0 ± 48.3	40.0 ± 51.6	60.0 ± 51.6	60.0 ± 51.6	20.0 ± 42.2	30.0 ± 48.3	70.0 ± 48.3	0.0 ± 0.0	60.0 ± 51.6	30.0 ± 48.3
	MLM	City Block	30.0 ± 48.3	40.0 ± 51.6	60.0 ± 51.6	50.0 ± 52.7	20.0 ± 42.2	50.0 ± 52.7	10.0 ± 31.6	10.0 ± 31.6	10.0 ± 31.6	20.0 ± 42.2
		Euclidean	10.0 ± 31.6	80.0 ± 42.2	80.0 ± 42.2	80.0 ± 42.2	20.0 ± 42.2	60.0 ± 51.6	30.0 ± 48.3	10.0 ± 31.6	30.0 ± 48.3	20.0 ± 42.2
		Mahalanobis	40.0 ± 51.6	80.0 ± 42.2	100.0 ± 0.0	60.0 ± 51.6	60.0 ± 51.6	70.0 ± 48.3	40.0 ± 51.6	60.0 ± 51.6	70.0 ± 48.3	50.0 ± 52.7
	MLM-NN	City Block	30.0 ± 48.3	40.0 ± 51.6	60.0 ± 51.6	50.0 ± 52.7	20.0 ± 42.2	50.0 ± 52.7	10.0 ± 31.6	10.0 ± 31.6	10.0 ± 31.6	20.0 ± 42.2
		Euclidean	10.0 ± 31.6	80.0 ± 42.2	80.0 ± 42.2	80.0 ± 42.2	20.0 ± 42.2	60.0 ± 51.6	30.0 ± 48.3	10.0 ± 31.6	30.0 ± 48.3	20.0 ± 42.2
		Mahalanobis	40.0 ± 51.6	80.0 ± 42.2	100.0 ± 0.0	60.0 ± 51.6	60.0 ± 51.6	70.0 ± 48.3	40.0 ± 51.6	60.0 ± 51.6	70.0 ± 48.3	50.0 ± 52.7
	MLP		40.0 ± 51.6	60.0 ± 51.6	90.0 ± 31.6	60.0 ± 51.6	30.0 ± 48.3	60.0 ± 51.6	40.0 ± 51.6	40.0 ± 51.6	30.0 ± 48.3	30.0 ± 48.3
	SVM	Linear	0.0 ± 0.0	40.0 ± 51.6	70.0 ± 48.3	30.0 ± 48.3	0.0 ± 0.0	20.0 ± 42.2	0.0 ± 0.0	0.0 ± 0.0	20.0 ± 42.2	0.0 ± 0.0
		RBF	40.0 ± 51.6	60.0 ± 51.6	50.0 ± 52.7	50.0 ± 52.7	30.0 ± 48.3	10.0 ± 31.6	50.0 ± 52.7	30.0 ± 48.3	40.0 ± 51.6	40.0 ± 51.6
Hu	Bayes	Normal	50.0 ± 52.7	40.0 ± 51.6	60.0 ± 51.6	80.0 ± 42.2	50.0 ± 52.7	60.0 ± 51.6	10.0 ± 31.6	50.0 ± 52.7	50.0 ± 52.7	20.0 ± 42.2
	LSSVM	Linear	0.0 ± 0.0	0.0 ± 0.0	10.0 ± 31.6	0.0 ± 0.0	0.0 ± 0.0	0.0 ± 0.0	0.0 ± 0.0	0.0 ± 0.0	0.0 ± 0.0	0.0 ± 0.0
		RBF	30.0 ± 48.3	50.0 ± 52.7	50.0 ± 52.7	30.0 ± 48.3	10.0 ± 31.6	40.0 ± 51.6	30.0 ± 48.3	40.0 ± 51.6	80.0 ± 42.2	30.0 ± 48.3
	MLM	City Block	10.0 ± 31.6	50.0 ± 52.7	30.0 ± 48.3	40.0 ± 51.6	40.0 ± 51.6	50.0 ± 52.7	20.0 ± 42.2	20.0 ± 42.2	0.0 ± 0.0	10.0 ± 31.6
		Euclidean	70.0 ± 48.3	70.0 ± 48.3	60.0 ± 51.6	60.0 ± 51.6	60.0 ± 51.6	50.0 ± 52.7	50.0 ± 52.7	40.0 ± 51.6	60.0 ± 51.6	40.0 ± 51.6
		Mahalanobis	50.0 ± 52.7	60.0 ± 51.6	80.0 ± 42.2	50.0 ± 52.7	50.0 ± 52.7	80.0 ± 42.2	60.0 ± 51.6	40.0 ± 51.6	40.0 ± 51.6	40.0 ± 51.6
	MLM-NN	City Block	10.0 ± 31.6	50.0 ± 52.7	30.0 ± 48.3	40.0 ± 51.6	40.0 ± 51.6	50.0 ± 52.7	20.0 ± 42.2	20.0 ± 42.2	0.0 ± 0.0	10.0 ± 31.6
		Euclidean	70.0 ± 48.3	70.0 ± 48.3	60.0 ± 51.6	60.0 ± 51.6	60.0 ± 51.6	50.0 ± 52.7	50.0 ± 52.7	40.0 ± 51.6	60.0 ± 51.6	40.0 ± 51.6
		Mahalanobis	50.0 ± 52.7	60.0 ± 51.6	80.0 ± 42.2	50.0 ± 52.7	50.0 ± 52.7	80.0 ± 42.2	60.0 ± 51.6	40.0 ± 51.6	40.0 ± 51.6	40.0 ± 51.6
	MLP		60.0 ± 51.6	40.0 ± 51.6	50.0 ± 52.7	20.0 ± 42.2	30.0 ± 48.3	40.0 ± 51.6	20.0 ± 42.2	40.0 ± 51.6	30.0 ± 48.3	40.0 ± 51.6
	SVM	Linear	0.0 ± 0.0	0.0 ± 0.0	20.0 ± 42.2	0.0 ± 0.0	0.0 ± 0.0	0.0 ± 0.0	0.0 ± 0.0	0.0 ± 0.0	0.0 ± 0.0	0.0 ± 0.0
		RBF	30.0 ± 48.3	50.0 ± 52.7	50.0 ± 52.7	30.0 ± 48.3	20.0 ± 42.2	40.0 ± 51.6	20.0 ± 42.2	40.0 ± 51.6	60.0 ± 51.6	30.0 ± 48.3
LBP	Bayes	Normal	10.0 ± 31.6	60.0 ± 51.6	80.0 ± 42.2	60.0 ± 51.6	90.0 ± 31.6	60.0 ± 51.6	50.0 ± 52.7	80.0 ± 42.2	80.0 ± 42.2	30.0 ± 48.3
	LSSVM	Linear	0.0 ± 0.0	40.0 ± 51.6	30.0 ± 48.3	30.0 ± 48.3	10.0 ± 31.6	0.0 ± 0.0	20.0 ± 42.2	20.0 ± 42.2	60.0 ± 51.6	0.0 ± 0.0
		RBF	70.0 ± 48.3	90.0 ± 31.6	90.0 ± 31.6	60.0 ± 51.6	100.0 ± 0.0	70.0 ± 48.3	80.0 ± 42.2	100.0 ± 0.0	100.0 ± 0.0	50.0 ± 52.7
	MLM	City Block	50.0 ± 52.7	80.0 ± 42.2	90.0 ± 31.6	60.0 ± 51.6	90.0 ± 31.6	70.0 ± 48.3	60.0 ± 51.6	80.0 ± 42.2	90.0 ± 31.6	70.0 ± 48.3
		Euclidean	50.0 ± 52.7	80.0 ± 42.2	100.0 ± 0.0	80.0 ± 42.2	90.0 ± 31.6	80.0 ± 42.2	80.0 ± 42.2	80.0 ± 42.2	90.0 ± 31.6	80.0 ± 42.2
		Mahalanobis	60.0 ± 51.6	90.0 ± 31.6	100.0 ± 0.0	80.0 ± 42.2	90.0 ± 31.6	90.0 ± 31.6	80.0 ± 42.2	80.0 ± 42.2	100.0 ± 0.0	90.0 ± 31.6
	MLM-NN	City Block	50.0 ± 52.7	80.0 ± 42.2	90.0 ± 31.6	60.0 ± 51.6	90.0 ± 31.6	70.0 ± 48.3	60.0 ± 51.6	80.0 ± 42.2	90.0 ± 31.6	70.0 ± 48.3
		Euclidean	50.0 ± 52.7	80.0 ± 42.2	100.0 ± 0.0	80.0 ± 42.2	90.0 ± 31.6	80.0 ± 42.2	80.0 ± 42.2	80.0 ± 42.2	90.0 ± 31.6	80.0 ± 42.2
		Mahalanobis	60.0 ± 51.6	90.0 ± 31.6	100.0 ± 0.0	80.0 ± 42.2	90.0 ± 31.6	90.0 ± 31.6	80.0 ± 42.2	80.0 ± 42.2	100.0 ± 0.0	90.0 ± 31.6
	MLP		50.0 ± 52.7	80.0 ± 42.2	90.0 ± 31.6	60.0 ± 51.6	90.0 ± 31.6	50.0 ± 52.7	50.0 ± 52.7	80.0 ± 42.2	70.0 ± 48.3	70.0 ± 48.3
	SVM	Linear	50.0 ± 52.7	80.0 ± 42.2	70.0 ± 48.3	60.0 ± 51.6	60.0 ± 51.6	20.0 ± 42.2	40.0 ± 51.6	60.0 ± 51.6	90.0 ± 31.6	30.0 ± 48.3
		RBF	70.0 ± 48.3	90.0 ± 31.6	100.0 ± 0.0	70.0 ± 48.3	70.0 ± 48.3	70.0 ± 48.3	70.0 ± 48.3	70.0 ± 48.3	100.0 ± 0.0	40.0 ± 51.6
Statistics M.	Bayes	Normal	70.0 ± 48.3	100.0 ± 0.0	90.0 ± 31.6	100.0 ± 0.0	70.0 ± 48.3	80.0 ± 42.2	80.0 ± 42.2	70.0 ± 48.3	80.0 ± 42.2	80.0 ± 42.2
	LSSVM	Linear	0.0 ± 0.0	0.0 ± 0.0	10.0 ± 31.6	0.0 ± 0.0	0.0 ± 0.0	0.0 ± 0.0	0.0 ± 0.0	0.0 ± 0.0	0.0 ± 0.0	0.0 ± 0.0
		RBF	40.0 ± 51.6	50.0 ± 52.7	80.0 ± 42.2	20.0 ± 42.2	50.0 ± 52.7	90.0 ± 31.6	90.0 ± 31.6	50.0 ± 52.7	100.0 ± 0.0	60.0 ± 51.6
	MLM	City Block	30.0 ± 48.3	50.0 ± 52.7	90.0 ± 31.6	20.0 ± 42.2	50.0 ± 52.7	30.0 ± 48.3	20.0 ± 42.2	50.0 ± 52.7	50.0 ± 52.7	20.0 ± 42.2
		Euclidean	60.0 ± 51.6	60.0 ± 51.6	70.0 ± 48.3	60.0 ± 51.6	50.0 ± 52.7	50.0 ± 52.7	40.0 ± 51.6	50.0 ± 52.7	80.0 ± 42.2	40.0 ± 51.6
		Mahalanobis	60.0 ± 51.6	100.0 ± 0.0	100.0 ± 0.0	60.0 ± 51.6	90.0 ± 31.6	70.0 ± 48.3	80.0 ± 42.2	60.0 ± 51.6	50.0 ± 52.7	60.0 ± 51.6
	MLM-NN	City Block	30.0 ± 48.3	50.0 ± 52.7	90.0 ± 31.6	20.0 ± 42.2	50.0 ± 52.7	30.0 ± 48.3	20.0 ± 42.2	50.0 ± 52.7	50.0 ± 52.7	20.0 ± 42.2
		Euclidean	60.0 ± 51.6	60.0 ± 51.6	70.0 ± 48.3	60.0 ± 51.6	50.0 ± 52.7	50.0 ± 52.7	40.0 ± 51.6	50.0 ± 52.7	80.0 ± 42.2	40.0 ± 51.6
		Mahalanobis	60.0 ± 51.6	100.0 ± 0.0	100.0 ± 0.0	60.0 ± 51.6	90.0 ± 31.6	70.0 ± 48.3	80.0 ± 42.2	60.0 ± 51.6	50.0 ± 52.7	60.0 ± 51.6
	MLP		60.0 ± 51.6	50.0 ± 52.7	60.0 ± 51.6	50.0 ± 52.7	80.0 ± 42.2	60.0 ± 51.6	40.0 ± 51.6	40.0 ± 51.6	40.0 ± 51.6	30.0 ± 48.3
	SVM	Linear	0.0 ± 0.0	20.0 ± 42.2	60.0 ± 51.6	20.0 ± 42.2	10.0 ± 31.6	10.0 ± 31.6	0.0 ± 0.0	10.0 ± 31.6	40.0 ± 51.6	0.0 ± 0.0
		RBF	40.0 ± 51.6	50.0 ± 52.7	70.0 ± 48.3	30.0 ± 48.3	40.0 ± 51.6	70.0 ± 48.3	60.0 ± 51.6	70.0 ± 48.3	100.0 ± 0.0	30.0 ± 48.3
	SIFT		30.0 ± 48.3	20.0 ± 42.2	20.0 ± 42.2	30.0 ± 48.3	10.0 ± 31.6	10.0 ± 31.6	10.0 ± 31.6	0.0 ± 0.0	0.0 ± 0.0	0.0 ± 0.0
	SURF		27.6 ± 45.9	18.9 ± 41.1	18.4 ± 40.6	28.9 ± 47.2	8.8 ± 30.4	7.4 ± 29.0	7.6 ± 29.2	0.0 ± 0.0	0.0 ± 0.0	0.0 ± 0.0

the K number of reference points ranged from 5% to 100% (step of 5) of the training set.

For SIFT and SURF, ten different random permutations of the images captured on virtual and real environments were taken, and one image of each class was chosen to create the training set and the remaining for the test set. SIFT was validated using kd-tree on matching function from the VLFeat library (Vedaldi & Fulkerson, 2008). The SURF matching function was based on the default settings in MATLAB (2013).

Table 5 shows the average and standard deviation values for specificity (Spc), sensitivity (Se), positive predictive value (PPV), f-score, harmonic means (HM) and accuracy (Acc) obtained by the machine learning techniques using the virtual environment. Likewise, Table 6 presents the results of the real environment. The experiments were computed on an iMac 2.5 GHz processor Core i5 with 4GB RAM.

Table 7 shows the accuracy and prediction time for a sample, that are important criteria for embedded applications. The best MLM, MLM-NN and Bayes classifiers are highlighted in

Table 10
Accuracy by route obtained from the feature extraction techniques and classifiers **with reject option**.

Feature	Classifier	Setup	Route 1	Route 2	Route 3	Route 4	Route 5	Route 6	Route 7	Route 8	Route 9	Route 10
Central M.	Bayes	Normal	100.0 ± 0.0	90.0 ± 31.6	100.0 ± 0.0	90.0 ± 31.6	90.0 ± 31.6	90.0 ± 31.6	70.0 ± 48.3	50.0 ± 52.7	100.0 ± 0.0	80.0 ± 42.2
	LSSVM	Linear	0.0 ± 0.0	0.0 ± 0.0	100.0 ± 0.0	0.0 ± 0.0	0.0 ± 0.0	60.0 ± 51.6	0.0 ± 0.0	0.0 ± 0.0	60.0 ± 51.6	0.0 ± 0.0
		RBF	70.0 ± 48.3	40.0 ± 51.6	100.0 ± 0.0	80.0 ± 42.2	70.0 ± 48.3	70.0 ± 48.3	70.0 ± 48.3	50.0 ± 52.7	100.0 ± 0.0	40.0 ± 51.6
	MLM	City Block	70.0 ± 48.3	60.0 ± 51.6	70.0 ± 48.3	40.0 ± 51.6	90.0 ± 31.6	80.0 ± 42.2	40.0 ± 51.6	40.0 ± 51.6	100.0 ± 0.0	60.0 ± 51.6
		Euclidean	80.0 ± 42.2	70.0 ± 48.3	100.0 ± 0.0	90.0 ± 31.6	60.0 ± 51.6	90.0 ± 31.6	90.0 ± 31.6	90.0 ± 31.6	100.0 ± 0.0	100.0 ± 0.0
		Mahalanobis	100.0 ± 0.0	70.0 ± 48.3	90.0 ± 31.6	90.0 ± 31.6	100.0 ± 0.0	90.0 ± 31.6	100.0 ± 0.0	80.0 ± 42.2	100.0 ± 0.0	90.0 ± 31.6
	MLM-NN	City Block	70.0 ± 48.3	60.0 ± 51.6	70.0 ± 48.3	40.0 ± 51.6	90.0 ± 31.6	80.0 ± 42.2	40.0 ± 51.6	40.0 ± 51.6	100.0 ± 0.0	60.0 ± 51.6
		Euclidean	80.0 ± 42.2	70.0 ± 48.3	100.0 ± 0.0	90.0 ± 31.6	60.0 ± 51.6	90.0 ± 31.6	90.0 ± 31.6	90.0 ± 31.6	100.0 ± 0.0	100.0 ± 0.0
		Mahalanobis	100.0 ± 0.0	70.0 ± 48.3	90.0 ± 31.6	90.0 ± 31.6	100.0 ± 0.0	90.0 ± 31.6	100.0 ± 0.0	80.0 ± 42.2	100.0 ± 0.0	90.0 ± 31.6
	MLP		90.0 ± 31.6	80.0 ± 42.2	80.0 ± 42.2	90.0 ± 31.6	60.0 ± 51.6	50.0 ± 52.7	70.0 ± 48.3	80.0 ± 42.2	80.0 ± 42.2	90.0 ± 31.6
	SVM	Linear	50.0 ± 52.7	90.0 ± 31.6	100.0 ± 0.0	60.0 ± 51.6	40.0 ± 51.6	70.0 ± 48.3	60.0 ± 51.6	20.0 ± 42.2	80.0 ± 42.2	60.0 ± 51.6
		RBF	60.0 ± 51.6	50.0 ± 52.7	90.0 ± 31.6	70.0 ± 48.3	70.0 ± 48.3	70.0 ± 48.3	60.0 ± 51.6	40.0 ± 51.6	90.0 ± 31.6	50.0 ± 52.7
GLCM	Bayes	Normal	20.0 ± 42.2	60.0 ± 51.6	50.0 ± 52.7	50.0 ± 52.7	30.0 ± 48.3	80.0 ± 42.2	30.0 ± 48.3	40.0 ± 51.6	40.0 ± 51.6	20.0 ± 42.2
	LSSVM	Linear	10.0 ± 31.6	30.0 ± 48.3	60.0 ± 51.6	20.0 ± 42.2	20.0 ± 42.2	20.0 ± 42.2	10.0 ± 31.6	20.0 ± 42.2	50.0 ± 52.7	20.0 ± 42.2
		RBF	60.0 ± 51.6	50.0 ± 52.7	90.0 ± 31.6	70.0 ± 48.3	50.0 ± 52.7	70.0 ± 48.3	70.0 ± 48.3	70.0 ± 48.3	70.0 ± 48.3	50.0 ± 52.7
	MLM	City Block	60.0 ± 51.6	60.0 ± 51.6	90.0 ± 31.6	80.0 ± 42.2	70.0 ± 48.3	70.0 ± 48.3	40.0 ± 51.6	20.0 ± 42.2	50.0 ± 52.7	50.0 ± 52.7
		Euclidean	70.0 ± 48.3	90.0 ± 31.6	100.0 ± 0.0	100.0 ± 0.0	70.0 ± 48.3	70.0 ± 48.3	50.0 ± 52.7	90.0 ± 31.6	60.0 ± 51.6	80.0 ± 42.2
		Mahalanobis	90.0 ± 31.6	90.0 ± 31.6	100.0 ± 0.0	100.0 ± 0.0	90.0 ± 31.6	90.0 ± 31.6	80.0 ± 42.2	100.0 ± 0.0	100.0 ± 0.0	80.0 ± 42.2
	MLM-NN	City Block	60.0 ± 51.6	60.0 ± 51.6	90.0 ± 31.6	80.0 ± 42.2	70.0 ± 48.3	70.0 ± 48.3	40.0 ± 51.6	20.0 ± 42.2	50.0 ± 52.7	50.0 ± 52.7
		Euclidean	70.0 ± 48.3	90.0 ± 31.6	100.0 ± 0.0	100.0 ± 0.0	70.0 ± 48.3	70.0 ± 48.3	50.0 ± 52.7	90.0 ± 31.6	60.0 ± 51.6	80.0 ± 42.2
		Mahalanobis	90.0 ± 31.6	90.0 ± 31.6	100.0 ± 0.0	100.0 ± 0.0	90.0 ± 31.6	90.0 ± 31.6	80.0 ± 42.2	100.0 ± 0.0	100.0 ± 0.0	80.0 ± 42.2
	MLP		80.0 ± 42.2	80.0 ± 42.2	100.0 ± 0.0	80.0 ± 42.2	60.0 ± 51.6	80.0 ± 42.2	70.0 ± 48.3	90.0 ± 31.6	70.0 ± 48.3	60.0 ± 51.6
	SVM	Linear	60.0 ± 51.6	60.0 ± 51.6	100.0 ± 0.0	70.0 ± 48.3	40.0 ± 51.6	80.0 ± 42.2	70.0 ± 48.3	20.0 ± 42.2	60.0 ± 51.6	60.0 ± 51.6
		RBF	60.0 ± 51.6	60.0 ± 51.6	70.0 ± 48.3	60.0 ± 51.6	50.0 ± 52.7	10.0 ± 31.6	60.0 ± 51.6	60.0 ± 51.6	60.0 ± 51.6	40.0 ± 51.6
Hu	Bayes	Normal	80.0 ± 42.2	80.0 ± 42.2	80.0 ± 42.2	90.0 ± 31.6	90.0 ± 31.6	80.0 ± 42.2	80.0 ± 42.2	80.0 ± 42.2	80.0 ± 42.2	80.0 ± 42.2
	LSSVM	Linear	30.0 ± 48.3	0.0 ± 0.0	90.0 ± 31.6	0.0 ± 0.0	10.0 ± 31.6	0.0 ± 0.0	20.0 ± 42.2	0.0 ± 0.0	0.0 ± 0.0	10.0 ± 31.6
		RBF	50.0 ± 52.7	60.0 ± 51.6	100.0 ± 0.0	80.0 ± 42.2	20.0 ± 42.2	80.0 ± 42.2	50.0 ± 52.7	60.0 ± 51.6	100.0 ± 0.0	50.0 ± 52.7
	MLM	City Block	60.0 ± 51.6	60.0 ± 51.6	60.0 ± 51.6	50.0 ± 52.7	60.0 ± 51.6	60.0 ± 51.6	40.0 ± 51.6	50.0 ± 52.7	40.0 ± 51.6	50.0 ± 52.7
		Euclidean	90.0 ± 31.6	80.0 ± 42.2	80.0 ± 42.2	80.0 ± 42.2	100.0 ± 0.0	90.0 ± 31.6	100.0 ± 0.0	70.0 ± 48.3	70.0 ± 48.3	90.0 ± 31.6
		Mahalanobis	100.0 ± 0.0	80.0 ± 42.2	100.0 ± 0.0	80.0 ± 42.2	100.0 ± 0.0	90.0 ± 31.6	80.0 ± 42.2	80.0 ± 42.2	80.0 ± 42.2	60.0 ± 51.6
	MLM-NN	City Block	60.0 ± 51.6	60.0 ± 51.6	60.0 ± 51.6	50.0 ± 52.7	60.0 ± 51.6	60.0 ± 51.6	40.0 ± 51.6	50.0 ± 52.7	40.0 ± 51.6	50.0 ± 52.7
		Euclidean	90.0 ± 31.6	80.0 ± 42.2	80.0 ± 42.2	80.0 ± 42.2	100.0 ± 0.0	90.0 ± 31.6	100.0 ± 0.0	70.0 ± 48.3	70.0 ± 48.3	90.0 ± 31.6
		Mahalanobis	100.0 ± 0.0	80.0 ± 42.2	100.0 ± 0.0	80.0 ± 42.2	100.0 ± 0.0	90.0 ± 31.6	80.0 ± 42.2	80.0 ± 42.2	80.0 ± 42.2	60.0 ± 51.6
	MLP		80.0 ± 42.2	50.0 ± 52.7	90.0 ± 31.6	40.0 ± 51.6	90.0 ± 31.6	60.0 ± 51.6	60.0 ± 51.6	70.0 ± 48.3	50.0 ± 52.7	80.0 ± 42.2
	SVM	Linear	40.0 ± 51.6	30.0 ± 48.3	90.0 ± 31.6	0.0 ± 0.0	30.0 ± 48.3	40.0 ± 51.6	50.0 ± 52.7	30.0 ± 48.3	20.0 ± 42.2	10.0 ± 31.6
		RBF	60.0 ± 51.6	60.0 ± 51.6	70.0 ± 48.3	50.0 ± 52.7	40.0 ± 51.6	60.0 ± 51.6	40.0 ± 51.6	50.0 ± 52.7	70.0 ± 48.3	50.0 ± 52.7
LBP	Bayes	Normal	70.0 ± 48.3	80.0 ± 42.2	90.0 ± 31.6	90.0 ± 31.6	100.0 ± 0.0	90.0 ± 31.6	80.0 ± 42.2	80.0 ± 42.2	100.0 ± 0.0	100.0 ± 0.0
	LSSVM	Linear	90.0 ± 31.6	100.0 ± 0.0	90.0 ± 31.6	80.0 ± 42.2	80.0 ± 42.2	80.0 ± 42.2	70.0 ± 48.3	90.0 ± 31.6	90.0 ± 31.6	80.0 ± 42.2
		RBF	80.0 ± 42.2	100.0 ± 0.0	100.0 ± 0.0	70.0 ± 48.3	100.0 ± 0.0	90.0 ± 31.6	80.0 ± 42.2	100.0 ± 0.0	100.0 ± 0.0	90.0 ± 31.6
	MLM	City Block	90.0 ± 31.6	80.0 ± 42.2	100.0 ± 0.0	100.0 ± 0.0	90.0 ± 31.6	100.0 ± 0.0	90.0 ± 31.6	80.0 ± 42.2	100.0 ± 0.0	90.0 ± 31.6
		Euclidean	80.0 ± 42.2	90.0 ± 31.6	100.0 ± 0.0	100.0 ± 0.0	100.0 ± 0.0	100.0 ± 0.0	80.0 ± 42.2	80.0 ± 42.2	100.0 ± 0.0	100.0 ± 0.0
		Mahalanobis	80.0 ± 42.2	90.0 ± 31.6	100.0 ± 0.0	100.0 ± 0.0	100.0 ± 0.0	90.0 ± 31.6	100.0 ± 0.0	100.0 ± 0.0	100.0 ± 0.0	100.0 ± 0.0
	MLM-NN	City Block	90.0 ± 31.6	80.0 ± 42.2	100.0 ± 0.0	100.0 ± 0.0	90.0 ± 31.6	100.0 ± 0.0	90.0 ± 31.6	80.0 ± 42.2	100.0 ± 0.0	90.0 ± 31.6
		Euclidean	80.0 ± 42.2	90.0 ± 31.6	100.0 ± 0.0	100.0 ± 0.0	100.0 ± 0.0	100.0 ± 0.0	80.0 ± 42.2	80.0 ± 42.2	100.0 ± 0.0	100.0 ± 0.0
		Mahalanobis	80.0 ± 42.2	90.0 ± 31.6	100.0 ± 0.0	100.0 ± 0.0	100.0 ± 0.0	90.0 ± 31.6	100.0 ± 0.0	100.0 ± 0.0	100.0 ± 0.0	100.0 ± 0.0
	MLP		90.0 ± 31.6	90.0 ± 31.6	100.0 ± 0.0	90.0 ± 31.6	100.0 ± 0.0	80.0 ± 42.2	90.0 ± 31.6	80.0 ± 42.2	90.0 ± 31.6	100.0 ± 0.0
	SVM	Linear	80.0 ± 42.2	100.0 ± 0.0	90.0 ± 31.6	90.0 ± 31.6	70.0 ± 48.3	70.0 ± 48.3	70.0 ± 48.3	90.0 ± 31.6	90.0 ± 31.6	70.0 ± 48.3
		RBF	80.0 ± 42.2	100.0 ± 0.0	100.0 ± 0.0	80.0 ± 42.2	80.0 ± 42.2	90.0 ± 31.6	80.0 ± 42.2	80.0 ± 42.2	100.0 ± 0.0	40.0 ± 51.6
Statistics M.	Bayes	Normal	80.0 ± 42.2	100.0 ± 0.0	100.0 ± 0.0	100.0 ± 0.0	90.0 ± 31.6	90.0 ± 31.6	90.0 ± 31.6	90.0 ± 31.6	90.0 ± 31.6	100.0 ± 0.0
	LSSVM	Linear	0.0 ± 0.0	20.0 ± 42.2	90.0 ± 31.6	20.0 ± 42.2	0.0 ± 0.0	80.0 ± 42.2	0.0 ± 0.0	0.0 ± 0.0	80.0 ± 42.2	30.0 ± 48.3
		RBF	60.0 ± 51.6	60.0 ± 51.6	90.0 ± 31.6	50.0 ± 52.7	70.0 ± 48.3	90.0 ± 31.6	90.0 ± 31.6	80.0 ± 42.2	100.0 ± 0.0	90.0 ± 31.6
	MLM	City Block	70.0 ± 48.3	70.0 ± 48.3	100.0 ± 0.0	40.0 ± 51.6	70.0 ± 48.3	70.0 ± 48.3	50.0 ± 52.7	50.0 ± 52.7	70.0 ± 48.3	50.0 ± 52.7
		Euclidean	60.0 ± 51.6	80.0 ± 42.2	90.0 ± 31.6	80.0 ± 42.2	70.0 ± 48.3	70.0 ± 48.3	80.0 ± 42.2	80.0 ± 42.2	80.0 ± 42.2	70.0 ± 48.3
		Mahalanobis	70.0 ± 48.3	100.0 ± 0.0	100.0 ± 0.0	100.0 ± 0.0	90.0 ± 31.6	90.0 ± 31.6	100.0 ± 0.0	100.0 ± 0.0	80.0 ± 42.2	100.0 ± 0.0
	MLM-NN	City Block	70.0 ± 48.3	70.0 ± 48.3	100.0 ± 0.0	40.0 ± 51.6	70.0 ± 48.3	70.0 ± 48.3	50.0 ± 52.7	50.0 ± 52.7	70.0 ± 48.3	50.0 ± 52.7
		Euclidean	60.0 ± 51.6	80.0 ± 42.2	90.0 ± 31.6	80.0 ± 42.2	70.0 ± 48.3	70.0 ± 48.3	80.0 ± 42.2	80.0 ± 42.2	80.0 ± 42.2	70.0 ± 48.3
		Mahalanobis	70.0 ± 48.3	100.0 ± 0.0	100.0 ± 0.0	100.0 ± 0.0	90.0 ± 31.6	90.0 ± 31.6	100.0 ± 0.0	100.0 ± 0.0	80.0 ± 42.2	100.0 ± 0.0
	MLP		60.0 ± 51.6	70.0 ± 48.3	90.0 ± 31.6	70.0 ± 48.3	90.0 ± 31.6	80.0 ± 42.2	60.0 ± 51.6	70.0 ± 48.3	60.0 ± 51.6	60.0 ± 51.6
	SVM	Linear	30.0 ± 48.3	60.0 ± 51.6	80.0 ± 42.2	50.0 ± 52.7	40.0 ± 51.6	80.0 ± 42.2	80.0 ± 42.2	50.0 ± 52.7	90.0 ± 31.6	70.0 ± 48.3
		RBF	50.0 ± 52.7	60.0 ± 51.6	70.0 ± 48.3	40.0 ± 51.6	60.0 ± 51.6	80.0 ± 42.2	80.0 ± 42.2	70.0 ± 48.3	100.0 ± 0.0	60.0 ± 51.6
	SIFT		80.0 ± 42.2	40.0 ± 51.6	40.0 ± 51.6	70.0 ± 48.3	10.0 ± 31.6	40.0 ± 51.6	50.0 ± 52.7	50.0 ± 52.7	30.0 ± 48.3	10.0 ± 31.6
	SURF		77.7 ± 39.9	38.9 ± 50.6	37.3 ± 48.9	67.1 ± 45.4	7.6 ± 29.3	37.5 ± 49.1	47.5 ± 50.2	48.2 ± 50.9	27.7 ± 46.0	8.7 ± 30.3

Tables 5 and 6. To achieve a better understanding of the results, Table 8 presents the metrics by class for all feature extraction techniques for the mean case obtained by these methods in both virtual and real environments.

Fig. 7 compares the general results, with and without reject option, obtained for the classifiers on ten routes (Table 2) by the feature extractor technique, furthermore, this figure shows the SIFT and SURF results. One route is considered correct if the vision-based classification system hit all classes along the way. Table 9 shows the hit rate detailed by the route without reject option. Likewise, Table 10 presents the hit rate with reject option.

We can see from Tables 5 and 6 that LBP was the best feature extraction technique in images of both environments. This result is expected due its properties. LBP is tolerant against variations of illumination and uses a local logic of extraction, which can work well in both case. In the real environment, the other highlighted methods were statistical and central moments. They do not take into account the shape of objects and adopt a statistical approach. In addition, central moments use the position of the object, but without the severity of Hu moments.

In general, quadratic classifiers (Bayes, SVM-RBF, LSSVM-RBF, MLP, MLM and MLM) had high accuracy, but we can highlight

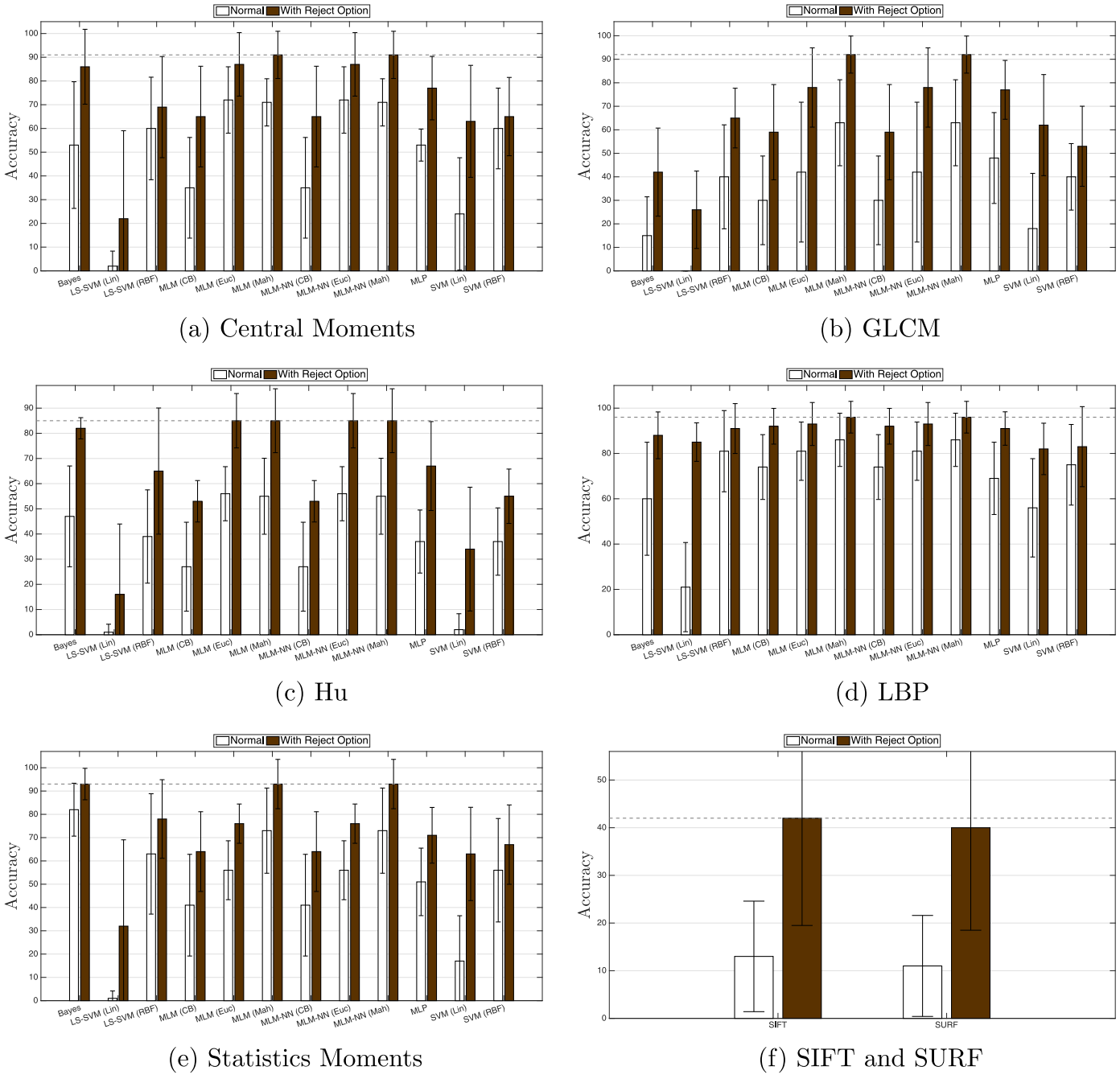

(a) Central Moments (b) GLCM

(c) Hu (d) LBP

(e) Statistics Moments (f) SIFT and SURF

Fig. 7. Average accuracy of route testing obtained by the feature extraction techniques and classifiers: normal and without reject option. We can see that our proposed method increases the accuracy in all cases. The detailed results are shown in Tables 9 and 10.

MLM and MLM-NN, using the three distance metrics, with accuracies greater than 99.9% in the virtual environment. Likewise in the real environment, MLM and MLM-NN, using the same distance metrics, obtained the best values with accuracies above 96.7%. LBP increases the accuracy of the linear classifiers, in other words, this feature extractor allows the problem to be separated linearly.

The fastest methods to train were the MLM, MLM-NN and Bayes and to test the latter two. As for the feature extraction method, the statistical moments was the fastest, followed by central moments, Hu moments, GLCM and LBP.

When we analyze the navigation results in Fig. 7, we can see that the best results of the feature extraction and machine learning techniques are the same as those shown in previous experiments. In addition, our proposed method for localization via classification with a reject option increases the accuracy in all cases. MLM-NN is able to speed up the MLM while maintaining accuracy. Furthermore, Mahalanobis distance is the metric with the highest accuracy in MLM and MLM-NN.

According to Tables 9 and 10, we show that the average gain was 15.83% per route using the method for localization via classification with a reject option. In general, our method achieves a significant improvement in accuracy. The MLM and MLM-NN along with LBP, for example, obtained 96% accuracy with our method, whereas in the previous situation the highest accuracy was 86%. Therefore, the proposed approach is shown to be useful and effective in mobile robot localization task with omnidirectional images.

7. Conclusion

In this work, we provided an evaluation of consolidated feature extractions and machine learning techniques in omnidirectional images focusing on topological map and localization tasks. In addition, we proposed a novel method for localization via classification with a reject option using omnidirectional images. This method increases the accuracy in all cases. Our experiments have demonstrated that LBP was the best feature extraction technique. This result was expected due its properties. Local visual features have better discriminative power, and are robust with respect to occlusion. Furthermore, good local visual features must be invariant to image rotation, image translation, image scale, changes of view, and even changes of illumination. Mahalanobis distance is the metric with the highest accuracy in MLM and MLM-NN in both environments. The fastest methods to train were the MLM, MLM-NN and Bayes and the fastest to test were the latter two. As regards the feature extraction method, the statistical and central moments were the fastest.

The main contributions are a novel method for localization via classification with reject option using omnidirectional images. The last is as the originality in using the feature extraction techniques based on moments, on texture, and keypoint descriptor along with a recently developed classifier for mobile robot localization task with omnidirectional images.

Another important contribution is the creation of two omnidirectional image data sets. Both can be used in other works to compare others localization and navigation techniques in this field.

Future work will include testing the vehicle in outdoor environments and other indoor environments. In addition, we will investigate other types of sensors with new mobile robots as well as other machine learning techniques such as the Optimum-Path Forest (OPF) (Nunes, Coelho, Lima, Papa, & de Albuquerque, 2014; Papa, Falcão, de Albuquerque, & Tavares, 2012) and feature extraction techniques such as the Structural Co-occurrence Matrix (SCM) (Ramalho, Ferreira, Filho, & de Medeiros, 2016). We will evaluate the system with reinforcement learning algorithms. Furthermore, feature selection techniques can be used to reduce dimensionality of the data. We will investigate the influence of image resolutions and other distance metrics used by MLM and MLM-NN. Finally, the system will be analyzed in tasks such as the museum guided tours, locations of trolleys in airports, and wheelchairs.

Acknowledgment

The first author acknowledge the sponsorship from the Cearense Foundation for the Support of Scientific and Technological Development (FUNCAP) by providing financial support. Victor Hugo C. de Albuquerque acknowledges the sponsorship from the Brazilian National Council for Research and Development (CNPq) via Grants 470501/2013-8 and 301928/2014-2. The last author acknowledges the sponsorship from the Federal Institute of Education, Science and Technology of Ceará, in Brazil, via the grants PROINFRA- IFCE/2013 and PROAPP-IFCE/2014.

References

Alarifi, A., Al-Salman, A., Alsaleh, M., Alnafessah, A., Al-Hadhrami, S., Al-Ammar, M. A., & Al-Khalifa, H. S. (2016). Ultra wideband indoor positioning technologies: Analysis and recent advances. *Sensors, 16*(5), 707.

Aldana-Murillo, N. G., Hayet, J.-B., & Becerra, H. M. (2015). Pattern recognition: 7th mexican conference, MCPR 2015. *Mexico City, Mexico, June 24–27, 2015, proceedings chapter Evaluation of Local Descriptors for Vision-Based Localization of Humanoid Robots* (pp. 179–189). Cham: Springer International Publishing.

Alves, M., Clua, E., & Leta, F. (2012). Evaluation of surface roughness standards applying haralick parameters and artificial neural networks. In *Systems, Signals and image processing (IWSSIP), 2012 19th International Conference on* (pp. 452–455).

Arbeiter, G., Bormann, R., Fischer, J., Hägele, M., & Verl, A. (2012). *Spatial cognition viii: International Conference, Spatial Cognition 2012, Kloster Seeon, Germany, August 31, – September 3, 2012. Proceedings* (pp. 114–127)). Berlin, Heidelberg: Springer Berlin Heidelberg.

de Azevedo, F. M., Brasil, L. M., & ao de Oliveira, R. C. L. (2000). *Redes neurais com aplições em controle e em sistemas especialistas*. Visual Books.

Bay, H., Ess, A., Tuytelaars, T., & Van Gool, L. (2008). Speeded-up robust features (surf). *Computer Vision and Image Understanding, 110*(3), 346–359.

Bengochea-Guevara, J. M., Conesa-Muñoz, J., Andújar, D., & Ribeiro, A. (2016). Merge fuzzy visual servoing and gps-based planning to obtain a proper navigation behavior for a small crop-inspection robot. *Sensors, 16*(3), 276.

Bessa, J. A., Barroso, D. A., da Rocha Neto, A. R., & de Alexandria, A. R. (2015). Global location of mobile robots using artificial neural networks in omnidirectional images. *IEEE Latin America Transactions, 13*(10), 3405–3414.

Beura, S., Majhi, B., & Dash, R. (2015). Mammogram classification using two dimensional discrete wavelet transform and gray-level co-occurrence matrix for detection of breast cancer. *Neurocomputing, 154*(0), 1–14.

Bonin-Font, F., Ortiz, A., & Oliver, G. (2008). Visual navigation for mobile robots: A survey. *Journal of Intelligent and Robotic Systems, 53*(3), 263.

Boroş, E., Roşca, G., & Iftene, A. (2010). *Multilingual information access evaluation ii. Multimedia Experiments: 10th Workshop of the Cross-Language Evaluation Forum, CLEF 2009, Corfu, Greece, September 30, - October 2, 2009, Revised Selected Papers* (pp. 277–282)). Berlin, Heidelberg: Springer Berlin Heidelberg.

Calderoni, L., Ferrara, M., Franco, A., & Maio, D. (2015). Indoor localization in a hospital environment using random forest classifiers. *Expert Systems with Applications, 42*(1), 125–134.

Campos, R. S., Lovisolo, L., & de Campos, M. L. R. (2014). Wi-fi multi-floor indoor positioning considering architectural aspects and controlled computational complexity. *Expert Systems with Applications, 41*(14), 6211–6223.

Caron, L.-C., Filliat, D., & Gepperth, A. (2015). *Computer vision - ECCV 2014 workshops: Zurich, Switzerland, September 6–7 and 12, 2014, Proceedings, Part III* (pp. 791–805)). Cham: Springer International Publishing.

Castellanos, J. A., & Tardos, J. D. (2012). *Mobile robot localization and map building: A multisensor fusion approach*. Springer Science & Business Media.

Charalampous, K., Kostavelis, L., & Gasteratos, A. (2015). Thorough robot navigation based on {SVM} local planning. *Robotics and Autonomous Systems, 70*, 166–180.

Cheng, H., Chen, H., & Liu, Y. (2015). Topological indoor localization and navigation for autonomous mobile robot. *Automation Science and Engineering, IEEE Transactions on, 12*(2), 729–738.

Chin, W. H., Loo, C. K., Seera, M., Kubota, N., & Toda, Y. (2016). Multi-channel bayesian adaptive resonance associate memory for on-line topological map building. *Applied Soft Computing, 38*, 269–280.

Chowdhury, T. J., Elkin, C., Devabhaktuni, V., Rawat, D. B., & Oluoch, J. (2016). Advances on localization techniques for wireless sensor networks: A survey. *Computer Networks, 110*, 284–305.

Chu, S., Hong, L., Liu, C., & Chen, J. (2014). A new regional shape index for classification of high resolution remote sensing images. In *Earth observation and remote sensing applications (EORSA), 2014 3rd International Workshop on* (pp. 156–160).

Cortes, C., & Vapnik, V. (1995). Support vector networks. *Machine Learning, 20*(3), 273–297.

Crammer, K., Singer, Y., Cristianini, N., Shawe-taylor, J., & Williamson, B. (2001). On the algorithmic implementation of multiclass kernel-based vector machines. *Journal of Machine Learning Research, 2*, 2001.

Cummins, M., & Newman, P. (2011). Appearance-only slam at large scale with fab-map 2.0. *The International Journal of Robotics Research, 30*(9), 1100–1123.

Czachorski, T., Kozielski, S., & Stanczyk, U. (2011). Man-machine interactions 2. *Advances in Intelligent and Soft Computing*. Springer Berlin Heidelberg.

Dawood, F., & Loo, C. K. (2015). Robot behaviour learning using topological gaussian adaptive resonance hidden markov model. *Neural Computing and Applications*, 1–14.

Deak, G., Curran, K., & Condell, J. (2012). A survey of active and passive indoor localisation systems. *Computer Communications, 35*(16), 1939–1954.

Debski, A., Grajewski, W., Zaborowski, W., & Turek, W. (2015). Open-source localization device for indoor mobile robots. *Procedia Computer Science, 76*, 139–146. 2015 {IEEE} International Symposium on Robotics and Intelligent Sensors (IEEE IRIS2015)

Dietterich, T. G., & Bakiri, G. (1995). Solving multiclass learning problems via error–correcting output codes. *Journal of Artificial Intelligence Research, 2*(1), 263–286.

Duan, K.-B., & Keerthi, S. (2005). Which is the best multiclass svm method? an empirical study. In N. Oza, R. Polikar, J. Kittler, & F. Roli (Eds.), *Multiple classifier systems*. In *Lecture notes in computer science: vol.3541* (pp. 278–285). Springer Berlin Heidelberg.

Duda, R. O., Hart, P. E., & Stork, D. G. (2000). *Pattern classification (2nd ed.)*. Wiley-Interscience.

Enrico, P., Groen, F., Arai, T., Dillmann, R., & Stenz, A. (2000). *Intelligent autonomous systems 6*. IOS Press.

Fang, S.-H., Wang, C.-H., Huang, T.-Y., Yang, C.-H., & Chen, Y.-S. (2012). An enhanced zigbee indoor positioning system with an ensemble approach. *IEEE Communications Letters, 16*(4), 564–567.

Flusser, J., Suk, T., Boldys, J., & Zitova, B. (2015). Projection operators and moment invariants to image blurring. *Pattern Analysis and Machine Intelligence, IEEE Transactions on, 37*(4), 786–802.

Fuentes-Pacheco, J., Ruiz-Ascencio, J., & Rendón-Mancha, J. M. (2015). Visual simultaneous localization and mapping: A survey. *Artificial Intelligence Review, 43*(1), 55–81.

Galvez-López, D., & Tardos, J. D. (2012). Bags of binary words for fast place recognition in image sequences. *IEEE Transactions on Robotics, 28*(5), 1188–1197.

Gamelas Sousa, R., Rocha Neto, A. R., Cardoso, J. S., & Barreto, G. A. (2015). Robust classification with reject option using the self-organizing map. *Neural Computing and Applications, 26*(7), 1603–1619.

Garcia-Fidalgo, E., & Ortiz, A. (2015). Vision-based topological mapping and localization methods. *Robotics and Autonomous Systems, 64*(C), 1–20.

Gerstmayr-Hillen, L., Röben, F., Krzykawski, M., Kreft, S., Venjakob, D., & Möller, R. (2013). Dense topological maps and partial pose estimation for visual control of an autonomous cleaning robot. *Robotics and Autonomous Systems, 61*(5), 497–516.

Gonzalez, R. C., & Woods, R. (2010). *Digital image processing* (3rd ed.). New Jersey: Pearson Prentice Hall.

Hafez, M. B., & Loo, C. K. (2015). Topological q-learning with internally guided exploration for mobile robot navigation. *Neural Computing and Applications, 26*(8), 1939–1954.

Haralick, R. (1979). Statistical and structural approaches to texture. *Proceedings of the IEEE, 67*(5), 786–804.

Hartmann, B. (2011). *Human worker activity recognition in industrial environments*. KIT Scientific Publishing.

Haykin, S. O. (2008). *Neural networks and learning machines*. Pearson Prentice Hall.

Hsieh, H. Y., & Chen, N. (2012). Recognising daytime and nighttime driving images using bayes classifier. *IET Intelligent Transport Systems, 6*(4), 482–493.

Hu, M.-K. (1962a). Visual pattern recognition by moment invariants. *Information Theory, IRE Transactions on, 8*(2), 179–187.

Hu, M.-K. (1962b). Visual pattern recognition by moment invariants. *Information Theory, IRE Transactions on, 8*(2), 179–187.

Jimenez, A. R., Seco, F., Prieto, C., & Guevara, J. (2009). A comparison of pedestrian dead-reckoning algorithms using a low-cost mems imu. In *Intelligent signal processing, 2009. WISP 2009. IEEE International Symposium On* (pp. 37–42).

Johns, E., & Yang, G.-Z. (2011). Global localization in a dense continuous topological map. In *Robotics and automation (ICRA), 2011 IEEE International Conference On* (pp. 1032–1037). IEEE.

Kang, T.-K., Choi, I.-H., & Lim, M.-T. (2015). MDGHM-SURF: A robust local image descriptor based on modified discrete gaussian —hermite moment. *Pattern Recognition, 48*(3), 670–684.

Kasat, N. R., & Thepade, S. D. (2016). Novel content based image classification method using {LBG} vector quantization method with bayes and lazy family data mining classifiers. *Procedia Computer Science, 79*, 483–489. Proceedings of International Conference on Communication, Computing and Virtualization (ICCCV) 2016

Kaushik, R., Bajaj, R. K., & Mathew, J. (2015). On image forgery detection using two dimensional discrete cosine transform and statistical moments. *Procedia Computer Science, 70*, 130–136. Proceedings of the 4th International Conference on Eco-friendly Computing and Communication Systems

Khan, Y. D., Ahmed, F., & Khan, S. A. (2013). Situation recognition using image moments and recurrent neural networks. *Neural Computing and Applications, 24*(7), 1519–1529.

Kim, H.-S., & Choi, J.-S. (2008). Advanced indoor localization using ultrasonic sensor and digital compass. In *Control, automation and systems, 2008. ICCAS 2008. International Conference On* (pp. 223–226). doi:10.1109/ICCAS.2008.4694553.

Kim, S., & Kweon, I. S. (2013). *Multimedia and ubiquitous engineering: MUE 2013* (pp. 975–981)). Dordrecht: Springer Netherlands.

Ko, N. Y., & Kuc, T.-Y. (2015). Fusing range measurements from ultrasonic beacons and a laser range finder for localization of a mobile robot. *Sensors, 15*(5), 11050.

Kothari, N., Kannan, B., Glasgwow, E. D., & Dias, M. B. (2012). Robust indoor localization on a commercial smart phone. *Procedia Computer Science, 10*, 1114–1120.

Kwiecień, A., Maćkowski, M., Kojder, M., & Manczyk, M. (2015). Reliability of bluetooth smart technology for indoor localization system. In P. Gaj, A. Kwiecień, & P. Stera (Eds.), *Computer Networks: 22nd International Conference, CN 2015, Brunów, Poland, June 16–19, 2015. Proceedings* (pp. 444–454)). Cham: Springer International Publishing.

Latif, M. A., Yusof, H. M., Sidek, S., & Rusli, N. (2015). Implementation of {GLCM} features in thermal imaging for human affective state detection. *Procedia Computer Science, 76*, 308–315. 2015 {IEEE} International Symposium on Robotics and Intelligent Sensors (IEEE IRIS2015)

Li, H. (2014). Low-cost 3d bluetooth indoor positioning with least square. *Wireless Personal Communications, 78*(2), 1331–1344.

Li, W., Dong, P., Xiao, B., & Zhou, L. (2016). Object recognition based on the region of interest and optimal bag of words model. *Neurocomputing, 172*, 271–280.

Licciardi, G., Villa, A., Dalla Mura, M., Bruzzone, L., Chanussot, J., & Benediktsson, J. (2012). Retrieval of the height of buildings from worldview-2 multi-angular imagery using attribute filters and geometric invariant moments. *Selected Topics in Applied Earth Observations and Remote Sensing, IEEE Journal of, 5*(1), 71–79.

Lim, H., Kung, L.-C., Hou, J. C., & Luo, H. (2010). Zero-configuration indoor localization over ieee 802.11 wireless infrastructure. *Wireless Networks, 16*(2), 405–420.

Liu, H. (2010). On the levenberg-marquardt training method for feed-forward neural networks. In *2010 sixth international conference on natural computation: 1* (pp. 456–460). doi:10.1109/ICNC.2010.5583151.

Liu, M., & Siegwart, R. (2012). Dp-fact: Towards topological mapping and scene recognition with color for omnidirectional camera. In *Robotics and automation (ICRA), 2012 IEEE International Conference On* (pp. 3503–3508).

Lowe, D. G. (2004). Distinctive image features from scale-invariant keypoints. *International Journal of Computer Vision*, 1–28.

Mainetti, L., Patrono, L., & Sergi, I. (2014). A survey on indoor positioning systems. In *Software, Telecommunications and Computer Networks (SoftCOM), 2014 22nd International Conference On* (pp. 111–120).

Maohai, L., Han, W., Lining, S., & Zesu, C. (2013). Robust omnidirectional mobile robot topological navigation system using omnidirectional vision. *Engineering Applications of Artificial Intelligence, 26*(8), 1942–1952.

MATLAB (2013). *Version 8.1.0 (R2013a)*. Natick, Massachusetts: The MathWorks Inc..

Mautz, R., & Tilch, S. (2011). Survey of optical indoor positioning systems. In *Indoor positioning and indoor navigation (IPIN), 2011 International Conference On* (pp. 1–7).

Mertzios, B. G. (1993). *Mutual impact of computing power and control theory* (pp. 281–287)). Boston, MA: Springer US.

Mesquita, D. P. P., Gomes, J. P. P., & Junior, A. H. S. (2015). Ensemble of minimal learning machines for pattern classification. In *Advances in computational intelligence - 13th international work-conference on artificial neural networks, IWANN 2015, Palma de Mallorca, Spain, June 10–12, 2015. Proceedings, Part II* (pp. 142–152).

Miah, M. S., & Gueaieb, W. (2011). A fuzzy logic approach for indoor mobile robot navigation using UKF and customized RFID communication. In M. Kamel, F. Karray, W. Gueaieb, & A. Khamis (Eds.), *Autonomous and Intelligent Systems: Second International Conference, AIS 2011, Burnaby, BC, Canada, June 22–24, 2011. Proceedings* (pp. 21–30)). Berlin, Heidelberg: Springer Berlin Heidelberg.

Miksik, O., Petyovsky, P., Zalud, L., & Jura, P. (2011). Robust detection of shady and highlighted roads for monocular camera based navigation of ugv. In *Robotics and automation (ICRA), 2011 IEEE International Conference On* (pp. 64–71).

Monica, S., & Ferrari, G. (2015). A swarm intelligence approach to 3d distance-based indoor uwb localization. In A. M. Mora, & G. Squillero (Eds.), *Applications of Evolutionary Computation: 18th European Conference, EvoApplications 2015, Copenhagen, Denmark, April 8–10, 2015, Proceedings* (pp. 91–102)). Cham: Springer International Publishing.

Morioka, H., Yi, S., & Hasegawa, O. (2011). Vision-based mobile robot's slam and navigation in crowded environments. In *2011 IEEE/RSJ International Conference on Intelligent Robots and Systems* (pp. 3998–4005).

Mozos, O. M., Mizutani, H., Kurazume, R., & Hasegawa, T. (2012). Categorization of indoor places using the kinect sensor. *Sensors, 12*(5), 6695–6711.

Nagla, K., Uddin, M., & Singh, D. (2012). Improved occupancy grid mapping in specular environment. *Robotics and Autonomous Systems, 60*(10), 1245–1252.

Niu, J., Ramana, K. V., Wang, B., & Rodrigues, J. J. P. C. (2014). *Ad-hoc, mobile, and wireless networks: 13th international conference, ADHOC-NOW 2014, Benidorm, SPAIN, june 22–27, 2014 Proceedings* (pp. 346–359)). Cham: Springer International Publishing.

Nowicki, M., & Skrzypczyński, P. (2015). Indoor navigation with a smartphone fusing inertial and wifi data via factor graph optimization. In S. Sigg, P. Nurmi, & F. Salim (Eds.), *Mobile Computing, Applications, and Services: 7th International Conference, MobiCASE 2015, Berlin, Germany, November 12–13, 2015, Revised Selected Papers* (pp. 280–298)). Cham

Nunes, T. M., Coelho, A. L., Lima, C. A., Papa, J. P., & de Albuquerque, V. H. C. (2014). {EEG} Signal classification for epilepsy diagnosis via optimum path forest a systematic assessment. *Neurocomputing, 136*, 103–123.

Ojala, T., Pietikainen, M., & Maenpaa, T. (2002). Multiresolution gray-scale and rotation invariant texture classification with local binary patterns. *Pattern Analysis and Machine Intelligence, IEEE Transactions on, 24*(7), 971–987.

Papa, J. P., FalcÃ£o, A. X., de Albuquerque, V. H. C., & Tavares, J. M. R. (2012). Efficient supervised optimum-path forest classification for large datasets. *Pattern Recognition, 45*(1), 512–520.

Paul, A., Bhattacharya, N., & Chowdhury, A. (2012a). Digit recognition from pressure sensor data using euler number and central moments. In *Communications, devices and intelligent systems (CODIS), 2012 International Conference On* (pp. 93–96).

Paul, A., Bhattacharya, N., & Chowdhury, A. S. (2012b). Digit recognition from pressure sensor data using euler number and central moments. In *Communications, devices and intelligent systems (CODIS), 2012 International Conference on* (pp. 93–96).

Piccinini, P., Prati, A., & Cucchiara, R. (2012). Real-time object detection and localization with sift-based clustering. *Image and Vision Computing, 30*(8), 573–587. Special Section: Opinion Papers

Platt, J. C., Cristianini, N., & Shawe-taylor, J. (2000). Large margin dags for multiclass classification. In *Advances in neural information processing systems* (pp. 547–553). MIT Press.

Rady, S. (2016). *Novel applications of intelligent systems* (pp. 231–250)). Cham: Springer International Publishing.

Raheja, J. L., Kumar, S., & Chaudhary, A. (2013). Fabric defect detection based on {GLCM} and gabor filter: A comparison. *Optik - International Journal for Light and Electron Optics, 124*(23), 6469–6474.

Ramalho, G. L. B., Ferreira, D. S., Filho, P. P. R., & de Medeiros, F. N. S. (2016). Rotation-invariant feature extraction using a structural co-occurrence matrix. *Measurement, 94*, 406–415.

Ranganathan, A., & Dellaert, F. (2011). Online probabilistic topological mapping. *The International Journal of Robotics Research*. 0278364910393287

Arias-de Reyna, E. (2013). A cooperative localization algorithm for uwb indoor sensor networks. *Wireless Personal Communications, 72*(1), 85–99.

Rituerto, A., Murillo, A., & Guerrero, J. (2014). Semantic labeling for indoor topological mapping using a wearable catadioptric system. *Robotics and Autonomous Systems, 62*(5), 685–695. Special Issue Semantic Perception, Mapping and Exploration

Rubio, F., Martínez-Gómez, J., Flores, M. J., & Puerta, J. M. (2016). Comparison between bayesian network classifiers and {SVMs} for semantic localization. *Expert Systems with Applications, 64*, 434–443.

de Sá Medeiros, C. M. (2008). *Uma Contribuição ao problema de seleção de modelos neurais usando o princiípio de máxima correlação dos erros*. Universidade Federal do Ceará Ph.D. thesis..

Saedan, M., Lim, C. W., & Ang, M. H. (2007). Appearance-based slam with map loop closing using an omnidirectional camera. In *2007 IEEE/ASME international conference on advanced intelligent mechatronics* (pp. 1–6).

Scaramuzza, D. (2014). *Computer vision: A reference guide* (pp. 552–560)). Boston, MA: Springer US.

Schindler, G., Metzger, C., & Starner, T. (2006). A wearable interface for topological mapping and localization in indoor environments. In M. Hazas, J. Krumm, & T. Strang (Eds.), *Location- and Context-Awareness: Second International Workshop, LoCA 2006, Dublin, Ireland, May 10–11, 2006. Proceedings* (pp. 64–73)). Berlin, Heidelberg: Springer Berlin Heidelberg.

Singh, K., Gupta, I., & Gupta, S. (2011). Classification of bamboo plant based on digital image processing by central moment. In *Image information processing (ICIIP), 2011 International Conference On* (pp. 1–5).

Singh, S., Maurya, R., & Mittal, A. (2012). Application of complete local binary pattern method for facial expression recognition. In *Intelligent human computer interaction (IHCI), 2012 4th International Conference on* (pp. 1–4).

Sioutis, M., & Tan, Y. (2014). User indoor location system with passive infrared motion sensors and space subdivision. In N. Streitz, & P. Markopoulos (Eds.), *Distributed, Ambient, and Pervasive Interactions: Second International Conference, DAPI 2014, Held as Part of HCI Interational 2014, Heraklion, Crete, Greece, June 22–27, 2014. Proceedings* (pp. 486–497)). Cham: Springer International Publishing.

Son, J., Kim, S., & Sohn, K. (2015). A multi-vision sensor-based fast localization system with image matching for challenging outdoor environments. *Expert Systems with Applications, 42*(22), 8830–8839. http://dx.doi.org/10.1016/j.eswa.2015.07.035.

Song, X., Gao, H., Ding, L., Deng, Z., & Chao, C. (2015). Diagonal recurrent neural networks for parameters identification of terrain based on wheel–soil interaction analysis. *Neural Computing and Applications*, 1–8.

Song, X., Li, X., Tang, W., & Zhang, W. (2016). A fusion strategy for reliable vehicle positioning utilizing {RFID} and in-vehicle sensors. *Information Fusion, 31*, 76–86.

Song, Z., Jiang, G., & Huang, C. (2011). *Theoretical and mathematical foundations of computer science: Second international conference, ICTMF 2011, Singapore, may 5–6, 2011. Selected papers* (pp. 198–206)). Berlin, Heidelberg: Springer Berlin Heidelberg.

de Souza Júnior, A. H., Corona, F., Barreto, G. A., Miche, Y., & Lendasse, A. (2015). Minimal learning machine: A novel supervised distance-based approach for regression and classification. *Neurocomputing, 164*, 34–44.

Suykens, J., & Vandewalle, J. (1999). Least squares support vector machine classifiers. *Neural Processing Letters, 9*(3), 293–300.

Sykora, P., Kamencay, P., & Hudec, R. (2014). Comparison of SIFT and SURF methods for use on hand gesture recognition based on depth map. *AASRI Procedia, 9*(0), 19–24. 2014 AASRI Conference on Circuit and Signal Processing (CSP 2014)

Theodoridis, S., & Koutroumbas, K. (2008). *Pattern recognition, Fourth edition* (4th). Academic Press.

Tsujinishi, D., & Abe, S. (2003). Fuzzy least squares support vector machines for multiclass problems. *Neural Networks, 16*(5–6), 785–792. Advances in Neural Networks Research: {IJCNN} '03

Vapnik, V. N. (1998). *Statistical learning theory*. John Wiley & Sons, Inc..

Varshavsky, A., de Lara, E., Hightower, J., LaMarca, A., & Otsason, V. (2007). {GSM} Indoor localization. *Pervasive and Mobile Computing, 3*(6), 698–720. PerCom 2007

Vedaldi, A., & Fulkerson, B. (2008). *VLFeat: An open and portable library of computer vision algorithms*.

Wang, Z. L., Cai, B. G., Yi, F. Z., & Li, M. (2012). *Advances in automation and robotics, vol. 2: Selected papers from the 2011 international conference on automation and robotics (ICAR 2011), Dubai, December 1–2, 2011* (pp. 593–601)). Berlin, Heidelberg: Springer Berlin Heidelberg.

Woo, J.-W., Lim, Y.-C., & Lee, M. (2010). Dynamic obstacle identification based on global and local features for a driver assistance system. *Neural Computing and Applications, 20*(7), 925–933.

Wu, H., hui Tian, G., Li, Y., yu Zhou, F., & Duan, P. (2014). Spatial semantic hybrid map building and application of mobile service robot. *Robotics and Autonomous Systems, 62*(6), 923–941.

Xu, R., Chen, W., Xu, Y., & Ji, S. (2015). A new indoor positioning system architecture using gps signals. *Sensors, 15*(5), 10074.

Yang, H., Shao, L., Zheng, F., Wang, L., & Song, Z. (2011a). Recent advances and trends in visual tracking: A review. *Neurocomputing, 74*(18), 3823–3831.

Yang, H.-Y., Wang, X.-Y., Wang, Q.-Y., & Zhang, X.-J. (2012). Ls-svm based image segmentation using color and texture information. *Journal of Visual Communication and Image Representation, 23*(7), 1095–1112.

Yang, J., Xiong, N., Vasilakos, A., Fang, Z., Park, D., Xu, X., … Yang, Y. (2011b). A fingerprint recognition scheme based on assembling invariant moments for cloud computing communications. *Systems Journal, IEEE, 5*(4), 574–583.

Yayan, U., Yucel, H., & Yazıcı, A. (2015). A low cost ultrasonic based positioning system for the indoor navigation of mobile robots. *Journal of Intelligent & Robotic Systems, 78*(3), 541–552.

Youssef, K., Argentieri, S., & Zarader, J. L. (2012). A binaural sound source localization method using auditive cues and vision. In *Acoustics, speech and signal processing (ICASSP), 2012 IEEE International Conference on* (pp. 217–220).

Zandian, R., & Witkowski, U. (2016). Performance analysis of small size and power efficient uwb communication nodes for indoor localization. In L. Alboul, D. Damian, & J. M. Aitken (Eds.), *Towards Autonomous Robotic Systems: 17th Annual Conference, TAROS 2016, Sheffield, UK, June 26–July 1, 2016, Proceedings* (pp. 371–382)). Cham: Springer International Publishing.

Zhang, H., Liu, Y., & Tan, J. (2015). Loop closing detection in rgb-d slam combining appearance and geometric constraints. *Sensors, 15*(6), 14639.

Zhang, Y., & Hua, C. (2015). Driver fatigue recognition based on facial expression analysis using local binary patterns. *Optik - International Journal for Light and Electron Optics, 126*(23), 4501–4505.

Zhu, L., Yang, A., Wu, D., & Liu, L. (2014). *Life system modeling and simulation: International conference on life system modeling and simulation, LSMS 2014, and international conference on intelligent computing for sustainable energy and environment, ICSEE 2014, Shanghai, China, September 20–23, 2014, Proceedings, part i* (pp. 400–409)). Berlin, Heidelberg: Springer Berlin Heidelberg.